blood

2012 120: 415-423
Prepublished online June 4, 2012;
doi:10.1182/blood-2011-12-399980

Calpain inhibition stabilizes the platelet proteome and reactivity in diabetes

Voahanginirina Randriamboavonjy, Johann Isaak, Amro Elgheznawy, Frank Pistrosch, Timo Frömel, Xiaoke Yin, Klaus Badenhoop, Heinrich Heide, Manuel Mayr and Ingrid Fleming

Blood (print ISSN 0006-4971, online ISSN 1528-0020), is published weekly by the American Society of Hematology, 2021 L St, NW, Suite 900, Washington DC 20036.

Calpain inhibition stabilizes the platelet proteome and reactivity in diabetes

*Voahanginirina Randriamboavonjy,[1] *Johann Isaak,[1] Amro Elgheznawy,[1] Frank Pistrosch,[2] Timo Frömel,[1] Xiaoke Yin,[3] Klaus Badenhoop,[4] Heinrich Heide,[5] Manuel Mayr,[3] and Ingrid Fleming[1]

[1]Institute for Vascular Signalling, Centre for Molecular Medicine, Goethe University, Frankfurt am Main, Germany; [2]Department of Medicine, Nephrology, University Hospital Carl Gustav Carus, Dresden, Germany; [3]King's British Heart Foundation Centre, King's College London, London, United Kingdom; [4]Department of Internal Medicine I, Division of Endocrinology, Goethe University, Frankfurt am Main, Germany; and [5]Molecular Bioenergetics Group, Goethe University, Frankfurt am Main, Germany

Platelets from patients with diabetes are hyperreactive and demonstrate increased adhesiveness, aggregation, degranulation, and thrombus formation, processes that contribute to the accelerated development of vascular disease. Part of the problem seems to be dysregulated platelet Ca^{2+} signaling and the activation of calpains, which are Ca^{2+}-activated proteases that result in the limited proteolysis of substrate proteins and subsequent alterations in signaling. In the present study, we report that the activation of μ- and m-calpain in patients with type 2 diabetes has profound effects on the platelet proteome and have identified septin-5 and the integrin-linked kinase (ILK) as novel calpain substrates. The calpain-dependent cleavage of septin-5 disturbed its association with syntaxin-4 and promoted the secretion of α-granule contents, including TGF-β and CCL5. Calpain was also released by platelets and cleaved CCL5 to generate a variant with enhanced activity. Calpain activation also disrupted the ILK-PINCH-Parvin complex and altered platelet adhesion and spreading. In diabetic mice, calpain inhibition reversed the effects of diabetes on platelet protein cleavage, decreased circulating CCL5 levels, reduced platelet-leukocyte aggregate formation, and improved platelet function. The results of the present study indicate that diabetes-induced platelet dysfunction is mediated largely by calpain activation and suggest that calpain inhibition may be an effective way of preserving platelet function and eventually decelerating atherothrombosis development. (*Blood*. 2012;120(2): 415-423)

Introduction

Calpains are Ca^{2+}-regulated cysteine proteases that are responsible for the limited proteolysis of target proteins, resulting in their modification (eg, activation, inhibition, or altered sensitivity to intracellular signals) rather than in their degradation.[1] In contrast to promiscuous degradative proteases, calpains cleave a relatively restricted set of protein substrates and use complex substrate recognition mechanisms involving primary and secondary structural features of target proteins to alter protein function and cellular signaling.[2]

Platelets express μ-calpain (calpain 1) and m-calpain (calpain 2); named for the micro- and millimolar Ca^{2+} concentrations, respectively, that are required to activate them in vitro.[3] Although Ca^{2+} is the main regulator of calpain activity, protease activation does not simply occur in response to any stimuli that increases platelet Ca^{2+}. Indeed, the regulation of proteolytic activity is complex and involves the association of calpain with a regulatory subunit, the endogenous inhibitor calpastatin,[4] other interacting proteins,[5] and binding to phospholipids.[6,7] Genetic deletion of m-calpain results in embryonic lethality,[8,9] but μ-calpain$^{-/-}$ mice are viable and demonstrate attenuated aggregation and clot retraction but normal bleeding times.[10] Mechanistically, the latter effects were attributed to the tyrosine dephosphorylation of platelet proteins because μ-calpain$^{-/-}$ platelets exhibited high levels of tyrosine phosphatase 1B protein and activity. Moreover, either an inhibitor of the phosphatase or the generation of μ-calpain–tyrosine phosphatase 1B double-knockout mice has been shown to rescue the platelet defect.[11] However, it is almost certain that the cleavage of a single phosphatase cannot account for the consequences of μ-calpain activation in platelets.

Pathophysiologically, the oxidative stress associated with type 2 diabetes results in the inactivation of the sarcoplasmic endoplasmic reticulum Ca^{2+} ATPase (SERCA-2) and a subsequent increase in platelet Ca^{2+} levels that is sufficient to activate calpain. This leads to the limited proteolysis of target proteins without eliciting full-blown platelet activation.[12] Several platelet proteins are known to be calpain substrates, including spectrin, adducin, talin, CD31, the myosin light-chain kinase, and N-ethylmaleimide-sensitive-factor attachment receptor (SNARE) proteins such as SNAP-23 and vesicle-associated membrane protein 3 (VAMP-3).[13] However, the spectrum of proteins that serve as pathophysiologically relevant targets of calpain in diabetic humans and their eventual role in the accelerated development of cardiovascular disease is unknown. Given that it is currently not possible to identify calpain targets on the basis of a specific recognition sequence, in the present study, we used a proteomic approach to identify novel calpain targets in diabetic platelets and to elucidate their role in platelet function. To determine which platelet proteins could be affected by calpain activation/inhibition in diabetic humans, we made use of the fact that peroxisome proliferator-activated receptor (PPAR)γ agonist therapy increases SERCA-2 expression, normalizes platelet Ca^{2+}, attenuates calpain activation, and prevents substrate cleavage.[12]

Submitted December 20, 2011; accepted May 24, 2012. Prepublished online as *Blood* First Edition paper, June 4, 2012; DOI 10.1182/blood-2011-12-399980.

*V.R. and J.I. contributed equally to this work.

The online version of this article contains a data supplement.

The publication costs of this article were defrayed in part by page charge payment. Therefore, and solely to indicate this fact, this article is hereby marked "advertisement" in accordance with 18 USC section 1734.

Methods

For full details of all methods, please see supplemental Methods (available on the *Blood* Web site; see the Supplemental Materials link at the top of the online article).

Pioglitazone study population

A total of 13 patients with type 2 diabetes mellitus were used in this study (5 women and 8 men; mean age, 47 ± 5.4 years; age range, 30-70 years; see supplemental Tables 1 and 2 for patient characteristics and medications). Patients were treated with either pioglitazone 30 mg/d (Actos; Takeda) or placebo each for 12 weeks in a cross-sectional design. There was a 4-week washout period between the different treatments. The study protocol was approved by the ethics committee of the Technical University of Dresden (number EK 233112006), and all of the participants gave written informed consent in accordance with the Declaration of Helsinki. Nondiabetic, age-matched subjects (7 women and 8 men; mean age, 40.25 ± 6.5 years; age range, 23-50 years; glycated hemoglobin (HbA_{1c}), 5.2% ± 0.6%; fasting plasma glucose, 5.1 ± 0.2mM) who had not taken any medication known to interfere with platelet aggregation for at least 10 days before the experiment served as the control group.

Diabetic study population

A total of 30 patients (16 women and 14 men; mean age, 47 ± 5.4 years; age range, 30-70 years) with type 2 diabetes mellitus attending the clinic for routine control visits were included in the study. Patients had to have HbA_{1c} more than 7.4% and fasting plasma glucose of 8.2 ± 0.7mM. All patients were treated with insulin alone or in combination with metformin. Nondiabetic, age-matched subjects (12 women and 18 men; mean age, 42.4 ± 4.5 years; age range, 25-65 years; HbA_{1c}, 5.2% ± 0.6%; fasting plasma glucose, 5.1 ± 0.2mM) who had not taken any medication known to interfere with platelet aggregation for at least 10 days before the experiment served as the control group. The study protocol was approved by the ethics committee of the Goethe University Hospital (number E 61/09 geschäfts number 86/09) and all of the participants gave written informed consent in accordance with the Declaration of Helsinki.

Animals

C57BL/6 mice (6-8 weeks of age) were from Charles River Laboratories. Floxed μ-calpain$^{-/-}$ mice (μ-cal$^{fl/fl}$) were generated by Taconic Artemis and bred with animals expressing the Cre deleter under the control of the PF4 promoter (The Jackson Laboratory) to generate mice lacking μ-calpain in platelets (PF4-μ-cal$^{-/-}$). Mice were housed in conditions that conform to the *Guide for the Care and Use of Laboratory Animals* published by the US National Institutes of Health (NIH publication no. 85-23). Both the university animal care committees and the Federal Authorities for Animal Research, Regierungspräsidium Darmstadt (Hessen, Germany; #F28/17) approved the study.

Diabetes was induced with a single IP injection of streptozotocin (150 mg/kg) and animals were considered diabetic when fasting plasma glucose was more than 250 mg/dL. In some experiments, animals were treated by oral gavage with the calpain inhibitor A-705253 (30 mg/kg/d) for 12 days after 12 weeks of untreated diabetes.

Statistical analysis

Data are expressed as means ± SEM and statistical evaluation was performed using the Student *t* test for unpaired data or 1-way ANOVA followed by a Bonferroni *t* test where appropriate using Prism 5 software (GraphPad). *P* values $< .05$ were considered statistically significant.

Results

Proteomic analysis of platelets from patients with and without pioglitazone therapy

Platelets were obtained from diabetic subjects before and after 12 weeks of therapy with pioglitazone (30 mg/d). Pioglitazone therapy increased insulin sensitivity (supplemental Table 1) and had profound effects on the platelet proteome (Figure 1A, supplemental Figure 1, supplemental Table 3). More than half of the differentially expressed protein spots identified were known calpain substrates (eg, talin-1 and filamin A)[13] and could be classified as cytoskeletal proteins and signaling molecules involved in metabolism and vesicle/secretory trafficking. Some of the proteins identified (eg, septin-5, the integrin-linked kinase [ILK] and glycerol-3-phosphate dehydrogenase 2 (GPD2) have not been previously linked with calpain.

To differentiate between calpain substrates and PPARγ-regulated genes, we determined the consequences of in vitro calpain activation on the levels of septin-5, ILK, and GPD2 in platelets from healthy subjects. Because platelet agonists alone are poor activators of the protease, calpains were activated via the Ca^{2+}-sensing receptor by increasing the extracellular concentration of Ca^{2+} as described previously[12] or using the combination of Ca^{2+} and ionomycin. The 2 approaches were also used to differentiate between μ- and m-calpain activation, both of which are expressed in platelets. In human platelets, extracellular Ca^{2+} was sufficient to stimulate the autolytic cleavage of μ-calpain and the limited degradation of septin-5 (Figure 1B). However, the combination of Ca^{2+} and ionomycin was required to activate m-calpain (decrease in latent m-calpain levels), which in turn resulted in the further degradation of septin-5 and ILK (Figure 1B). Because all of these changes were sensitive to the calpain inhibitor calpeptin, they could be attributed to calpain activation. GPD2 was unaffected by calpain activation, an observation that fits well with its classification as a PPARγ-regulated gene.[14] We also confirmed that levels of septin-5 and ILK were reduced in diabetic versus healthy subjects and increased as a result of pioglitazone therapy, which also reduced μ- and m-calpain activation (Figure 1C).

Because calpain inhibitors are not able to differentiate between μ- and m-calpain, we studied the sensitivity of septin-5 and ILK to Ca^{2+}-induced, calpain-mediated cleavage in mice lacking μ-calpain in platelets (PF4-μ-calpain$^{-/-}$ mice). The limited proteolysis of septin-5 was observed in Ca^{2+}-stimulated platelets from μ-cal$^{fl/fl}$ mice, but not their PF4-μ-cal$^{-/-}$ littermates (Figure 1D arrow). The combination of Ca^{2+} and ionomycin resulted in the further degradation of septin-5 (Figure 1D arrowhead) and was equally effective in μ-cal$^{fl/fl}$ and PF4-μ-cal$^{-/-}$ mice. Conversely, the degradation of ILK was only observed in platelets treated with Ca^{2+} and ionomycin, and was unaffected by the platelet-specific down-regulation of μ-calpain.

Calpain-dependent cleavage of septin-5 increases α-granule secretion

Septin-5 is a cytosolic GTP-binding protein that inhibits platelet degranulation by binding the SNARE protein syntaxin-4.[15] Septin-5 associated with syntaxin-4 in unstimulated platelets, but not after calpain activation with Ca^{2+} or the combination of Ca^{2+} and thrombin (Figure 2A). Conversely, calpain inhibition enhanced the syntaxin-4/septin-5 association. To determine the consequences of this interaction on platelet degranulation, we assayed the release of

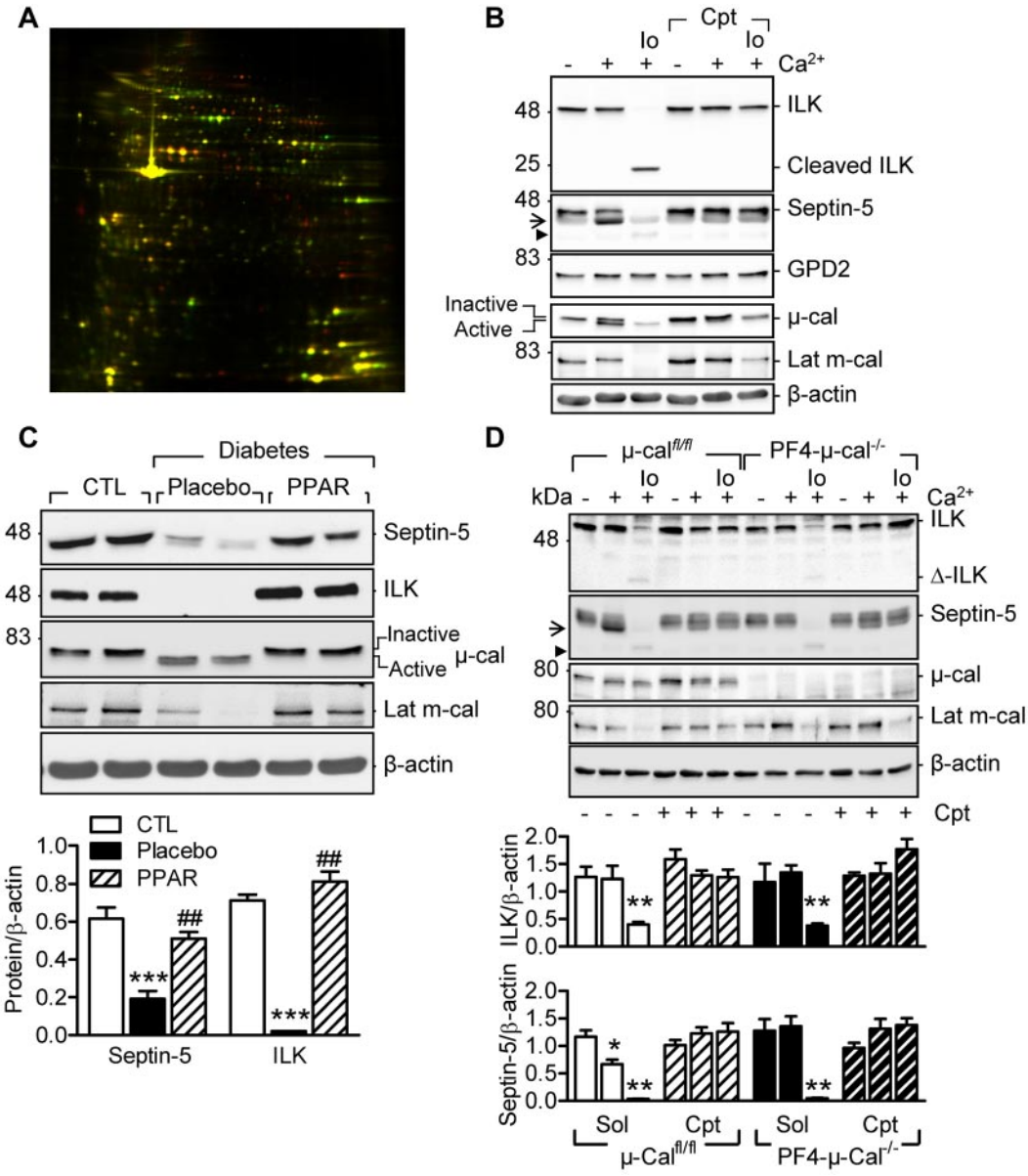

Figure 1. Characterization of new calpain substrates in human and murine platelets. (A) Representative differential in-gel electrophoresis of platelet proteins from the same diabetic patient treated with placebo or pioglitazone (red spots indicate proteins down-regulated by pioglitazone; green spots, proteins that were up-regulated). (B) Representative blots showing the effect of Ca^{2+} (5mM) and ionomycin (Io; 1μM)–induced μ- and m-calpain activation on the levels of septin-5, ILK, and GPD2 in washed human platelets. (C) Levels of septin-5 and ILK in washed platelets from healthy donors (CTL) and patients with type 2 diabetes treated with placebo or pioglitazone (PPAR) (data shown from same patients). (D) Effect of μ- and m-calpain activation on septin-5 and ILK in platelets from μ-cal$^{fl/fl}$ and PF4-μ-cal$^{-/-}$ mice. Experiments were performed in the absence or in the presence of calpeptin (Cpt, 10μM). Arrow indicates the product after μ-calpain activation; arrowhead, product after m-calpain activation. Blots are representative of 5-6 additional experiments and graphs summarize data obtained in 8 subjects/animals per group. *$P < .05$; **$P < .001$; ***$P < .001$ versus healthy donors or untreated platelets; ###$P < .001$ versus placebo.

the dense granule marker serotonin and the α-granule protein TGF-β in the absence and presence of Ca^{2+} and thrombin. Serotonin release was stimulated by thrombin, but was not affected by calpain activation/inactivation (Figure 2B), whereas thrombin was able to stimulate TGF-β release only after Ca^{2+}–induced calpain activation and not in the presence of the calpain inhibitor. Therefore, a calpain-sensitive process such as the cleavage of septin-5 seems to promote the release of α-granule contents actively.

CCL5 (RANTES) is a chemokine stored in α-granules that can be deposited onto the endothelium, where it attracts monocytes and can promote the development of vascular disease.[16] In contrast to TGF-β, small amounts of CCL5 were released from thrombin-stimulated platelets, but calpain activation increased CCL5 release significantly, whereas calpeptin inhibited it (Figure 2C). Moreover, circulating CCL5 was increased in plasma from diabetic subjects (Figure 2D), and more CCL5 was deposited by Ca^{2+}-activated platelets onto endothelial cells (Figure 2E).

Cleavage of CCL5 by μ-calpain enhances chemotactic activity

Calpain activation in human platelets also resulted in CCL5 cleavage (Figure 3A). The latter phenomenon could be confirmed in vitro using the recombinant protein and resulted in the generation of a variant with enhanced monocyte chemotactic activity (Figure 3B). To identify the CCL5 variant generated by μ-calpain,

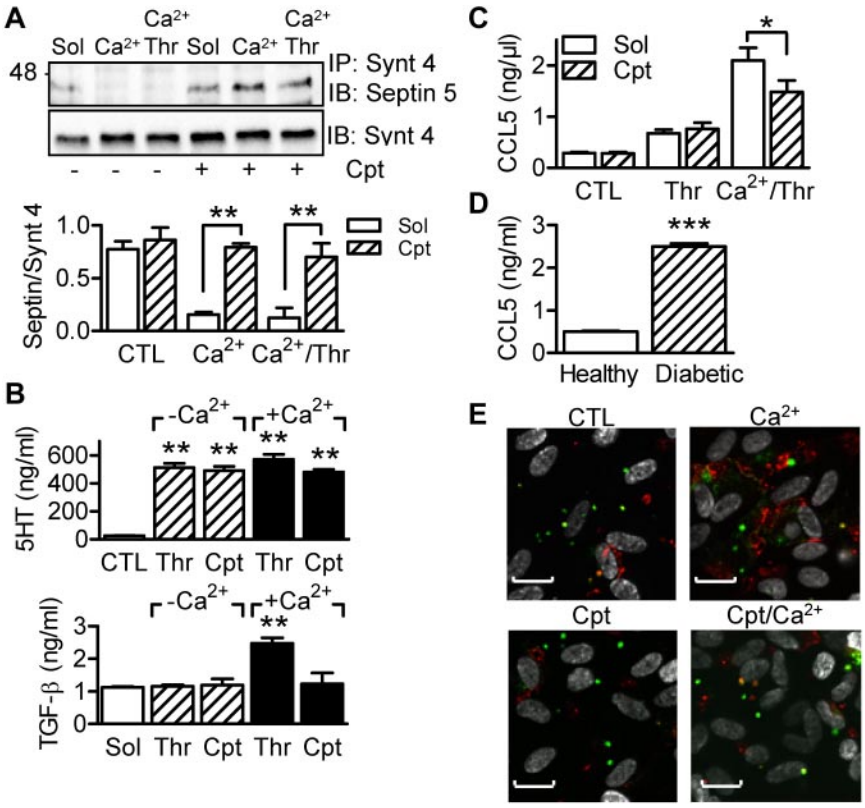

Figure 2. Calpain, septin-5, and platelet secretion. (A) Effect of calpain activation on the association of septin-5 with syntaxin-4 (Synt 4) in human platelets. (B) Levels of serotonin (5-HT) and TGF-β (ELISA) released from human platelets stimulated with either thrombin (Thr, 1 U/mL) or thrombin plus Ca^{2+} (to activate calpain). Experiments were performed in the absence and presence of calpeptin (Cpt, 10μM). (C) CCL5 levels in releasate from unstimulated and thrombin-stimulated platelets without and with calpain activation with Ca^{2+}. Experiments were performed in the absence or in the presence of calpeptin (Cpt). (D) Effect of diabetes on CCL5 levels (ELISA) in plasma from healthy subjects and from patients with type 2 diabetes. (E) Immunostaining of CCL5 (red) released from platelets (β3 integrin [green]) onto endothelial cells (DAPI; white). Platelets were either left unstimulated (CTL) or treated with Ca^{2+} in the absence or in the presence of calpeptin (Cpt). Bars represent 20μM. The graphs summarize data obtained with 5-6 subjects per group. $^*P < .05$, $^{**}P < .01$, $^{***}P < .001$ versus CTL/Sol/Healthy.

platelet-derived CCL5 and recombinant CCL5 protein were exposed to μ-calpain in vitro and then subjected to mass spectrometry. These experiments identified the peptide YSSDTTPCCFAYIARPLPR (supplemental Figure 2), representing residues 3-21, suggesting that μ-calpain cleaves CCL5 at the 2 first N-terminal amino acids and at a C-terminal position.

Calpain-mediated CCL5 cleavage may take place either in α-granules or in the extracellular space after its release. We found that μ-calpain was secreted from thrombin-stimulated platelets (Figure 3C), a finding that fits well with a recent report that identified calpain in the platelet secretome.[17] Indeed, calpain activity was measurable in plasma from healthy subjects and was

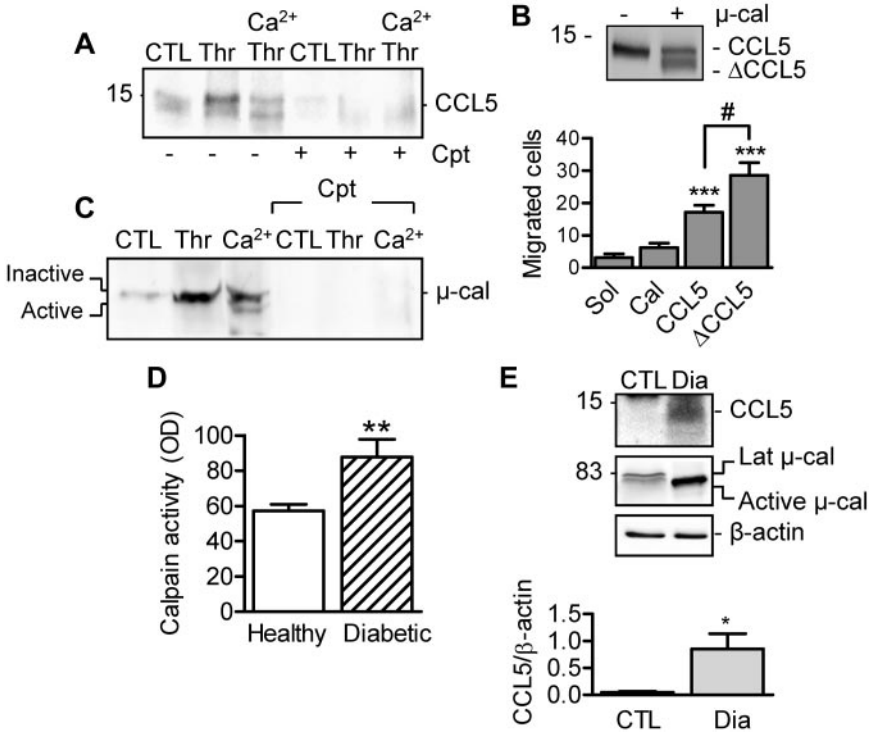

Figure 3. Effect of calpain-mediated cleavage on CCL5 activity. (A) CCL5 release and cleavage after calpain activation in the absence and presence of calpeptin (Cpt, 10μM). (B) Cleavage of recombinant CCL5 by μ-calpain and chemotactic activity of full-length and calpain-cleaved CCL5 (ΔCCL5) on THP-1 cells in a Transwell chamber. (C) μ-calpain in releasates from resting platelets or platelets activated with thrombin alone or after stimulation with Ca^{2+} (5mM, 30 minutes) in the absence or in the presence of calpeptin (Cpt). (D) Calpain activity in plasma from healthy subjects and from patients with type 2 diabetes. (E) CCL5 and μ-calpain in circulating microparticles isolated from healthy subjects (CTL) and patients with type 2 diabetes (Dia). The graphs summarize data obtained with 5-6 subjects per group. $^*P < .05$; $^{**}P < .01$; $^{***}P < .001$ versus CTL/Sol; #$P < .05$ versus full-length CCL5.

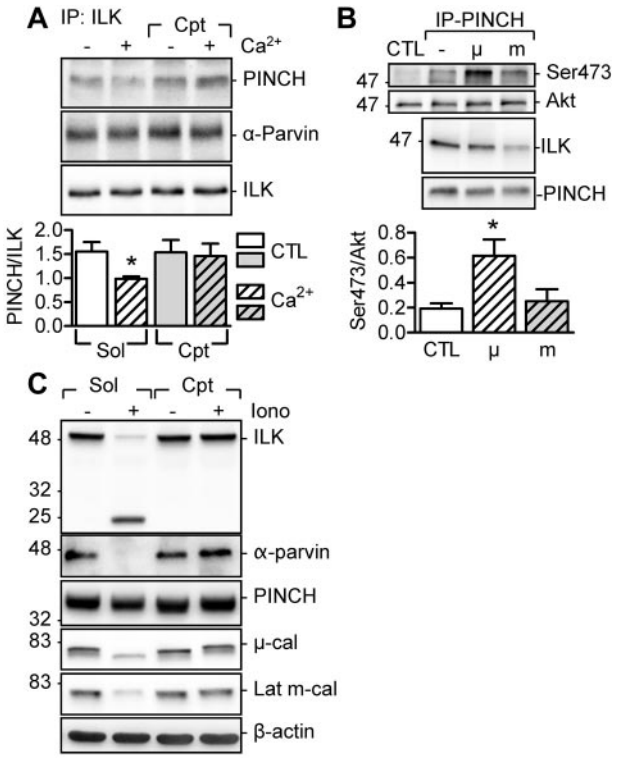

Figure 4. Effect of calpain activation on ILK. (A) Effect of Ca^{2+} with or without calpeptin (Cpt, 10μM) on the association of PINCH and α-Parvin with ILK. (B) Effect of purified μ- and m-calpain on the ability of PINCH-ILK complexes to phosphorylate Akt (on Ser-473) in washed human platelets. (C) Consequences of calpain activation by ionomycin (Iono, 1μM) on the levels of ILK, α-Parvin, and PINCH in washed human platelets. Identical results were obtained in 4 additional experiments. The graphs summarize data obtained with 5-6 subjects per group. *$P < .05$ versus CTL/Sol.

increased significantly in plasma from diabetic patients (Figure 3D). Moreover, whereas only latent (inactive) μ-calpain was detected in circulating microparticles from nondiabetic subjects, active μ-calpain and high levels of CCL5 were detected in samples from diabetic subjects (Figure 3E).

μ-calpain activation disrupts the ILK-PINCH-Parvin complex and promotes ILK activation

The second novel calpain substrate we identified was ILK. ILK forms the so-called ILK-PINCH-Parvin (IPP) complex, which is part of the focal adhesion complex and functions as a regulator of several signaling pathways.[18] We found that PINCH and α-Parvin were coprecipitated with the ILK from unstimulated platelets, and the Ca^{2+}-induced activation of μ-calpain resulted in the calpeptin-sensitive disassociation of PINCH from the kinase (Figure 4A). To determine the consequences of calpain activation on ILK activity, we assessed the ability of PINCH-ILK complexes to phosphorylate the ILK substrate Akt.[19,20] The ILK that coprecipitated with PINCH from untreated human platelets and added to unstimulated platelet lysates elicited a moderate phosphorylation of Akt. However, when the coprecipitate was treated with μ-calpain to disassociate ILK from PINCH, Akt phosphorylation increased. Conversely, incubation of the immunoprecipitates with m-calpain resulted in the degradation of ILK and failed to elicit Akt phosphorylation (Figure 4B). In vitro stimulation of washed human platelets with ionomycin to activate both calpain isoforms led to the cleavage of ILK and α-Parvin, but did not affect the level of PINCH significantly, suggesting that, in addition to ILK, α-Parvin is also an m-calpain substrate (Figure 4C). The cleavage of both proteins was prevented by calpeptin. Therefore, μ-calpain activation promotes the release of active ILK from the IPP complex, whereas the activation of m-calpain degrades 2 of the IPP proteins.

Differential contribution of μ- and m-calpain to platelet adhesion and spreading

The IPP complex assembles in the cytoplasm and is recruited subsequently to focal adhesions.[21] Therefore, we next focused on the role of calpain in regulating focal adhesion proteins and platelet adhesion and spreading. Indeed, 2 additional kinases linked to focal adhesion contacts, focal adhesion kinase (FAK) and proline-rich tyrosine kinase 2 (PYK2), were also attenuated in platelets from diabetic subjects (Figure 5A) and cleaved by calpain in vitro (Figure 5B). This is important because the proteolysis of focal adhesion proteins such as talin, paxillin (both are calpain substrates), and FAK is known to regulate focal adhesion dynamics and cell migration.[22,23]

In platelets from healthy subjects, Ca^{2+}-induced calpain activation increased the number of platelets that adhered to fibronectin in a calpeptin-sensitive manner (Figure 5C). Similar responses were observed in platelets from μ-$cal^{fl/fl}$ but not from PF4-μ-$cal^{-/-}$ mice (Figure 5D), suggesting a role for μ-calpain in platelet adhesion. Moreover, in platelets from healthy subjects, extracellular Ca^{2+} promoted lamellipodia formation and platelet spreading on fibronectin. The latter response was reduced in the presence of calpeptin in platelets from μ-$cal^{fl/fl}$ and PF4-μ-$cal^{-/-}$ mice (Figure 5E). Therefore, m-calpain rather than μ-calpain seems to be activated during platelet spreading.

Calpain inhibition reverses diabetes-associated platelet hyperactivation

Our next step was to determine the effects of calpain inhibition on platelet function. In platelets from healthy subjects, the calpain inhibitors calpeptin and A-705253[24] had moderate inhibitory effects on the thrombin-induced mobilization of Ca^{2+} and no significant effect on subsequent aggregation, but did attenuate clot retraction (supplemental Figure 3A-C). Both compounds prevented the Ca^{2+}-induced cleavage of CD31, but the mechanisms of action were distinct: whereas calpeptin prevented the autolytic cleavage of μ-calpain, A705253 did not (supplemental Figure 3D).

Given that calpain is activated by redox stress and calpain inhibition had little effect on agonist-induced responses, we hypothesized that calpain treatment may preserve platelet function in a mouse model of diabetes. As with platelets from patients with type 2 diabetes, diabetes in wild-type mice (12 weeks after streptozotocin treatment) resulted in the activation of μ- and m-calpain and a reduction in levels of septin-5, ILK, FAK, and PYK2. Treating animals over 12 days with A-705253 (30 mg/kg/d orally) had no effect on blood glucose or bleeding times (supplemental Figure 4), but was sufficient to increase levels of latent μ- and m-calpain and increase the levels of their substrates to those observed in nondiabetic mice (Figure 6A).

As with the human subjects, diabetes increased levels of CCL5 detected in circulating murine microparticles (Figure 6B), and this response was reversed in animals treated with A-705253. CCL5 was also deposited onto endothelial cells in the carotid arteries of diabetic mice, a phenomenon reduced by the calpain inhibitor (supplemental Figure 5).

Diabetes also accelerated thrombus formation after $FeCl_3$-induced carotid artery injury (the time to reach maximum size was

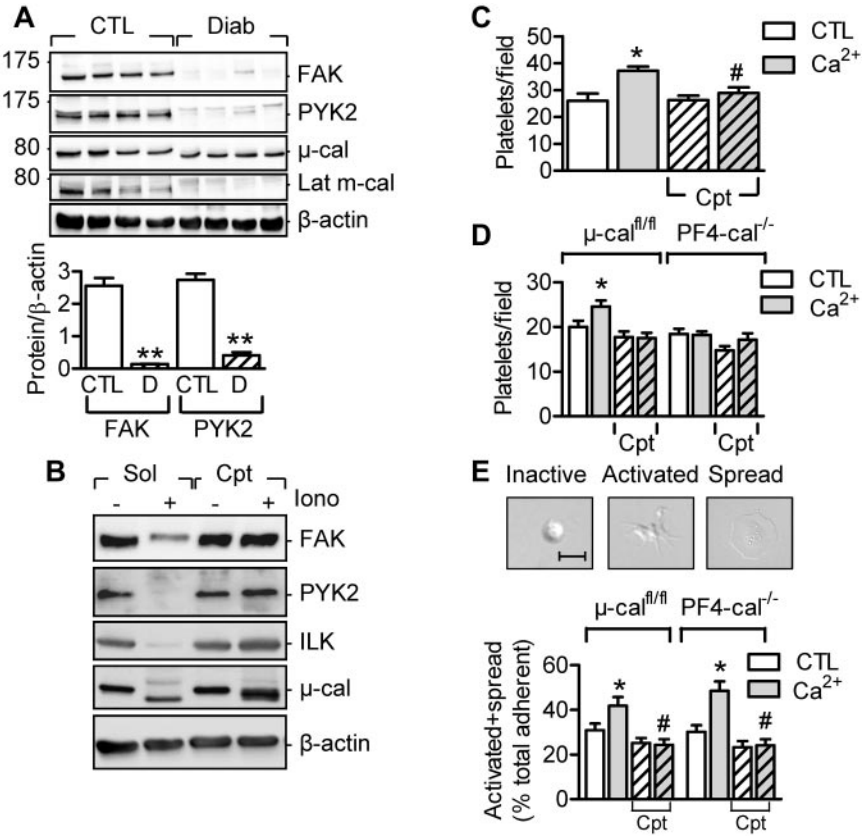

Figure 5. Role of calpain in platelet adhesion and spreading. (A) Levels of FAK and PYK2 in washed platelets from healthy subjects (CTL) and from patients with type 2 diabetes (Diab/D) and activated μ- and m-calpain. (B) FAK, PYK2, and ILK are calpain substrates in vitro. Washed human platelets were treated with either solvent or ionomycin in the absence (Sol) and presence of calpeptin (Cpt, 10μM). (C) Adherence of human platelets pre-treated with and without Ca^{2+} in the absence or in the presence of calpeptin (Cpt) to fibronectin-coated slides. (D) Adherence of platelets from μ-$cal^{fl/fl}$ or PF4-μ-$Cal^{-/-}$ mice pretreated with and without Ca^{2+} in the absence or in the presence of calpeptin (Cpt). (E) Effect of calpain inhibition on numbers of activated and spread platelets after stimulation of washed platelets from μ-$cal^{fl/fl}$ and PF4-μ-$Cal^{-/-}$ mice with Ca^{2+} in the absence or in the presence of calpeptin (Cpt). The graphs summarize data obtained in platelets from 4-5 subjects or 6-9 animals per group. *$P < .05$; **$P < .01$ versus control; #$P < .05$ versus Ca^{2+}-stimulated platelets without calpeptin.

17.5 ± 1.2 minutes in healthy versus 7.5 ± 0.4 minutes in diabetic mice, n = 8 per group, $P < .001$; Figure 6C), potentiated the formation of leukocyte-platelet aggregates in vivo (Figure 6D), and enhanced thrombin-induced platelet aggregation in vitro (Figure 6E). Whereas thrombus formation in vivo in nondiabetic mice was unaffected by calpain inhibition, A-705253 reduced the maximum thrombus size and decelerated thrombus formation (time to maximum was increased from 7.5 ± 0.4 [n = 8] to 14.7 ± 2.4 minutes in the A-705253–treated diabetic mice [n = 7]; $P < .05$; Figure 6C), reversed the diabetes-induced formation of leukocyte-platelet aggregates in vivo (Figure 6D), and attenuated thrombin-induced platelet aggregation (Figure 6E).

Discussion

The results of the present study identified septin-5 and the ILK as novel calpain substrates in diabetic platelets and linked the proteolysis of these proteins to the increased secretion and modification of the α-granule protein CCL5 and to altered platelet adhesion and spreading. Moreover, it was possible to reproduce the findings using human platelets in a mouse model of diabetes and to prevent the in vivo proteolysis of the substrates identified using a calpain inhibitor. Calpain inhibition was also shown to reverse the hyperreactivity observed in diabetic platelets and the formation of platelet-leukocyte aggregates.

Over the past 10 years, it has become clear that platelets are not simply involved in aggregation and clot formation, but that they also play an active role in vascular homoeostasis, largely by delivering an impressive array of vasoactive substances. Little is known about the changes in platelets that lead to the enhanced deposition of chemokines such as stromal cell-derived factor-1,[25] PF4, or CCL5[26] on the endothelial surface, which in turn promote the recruitment of circulating cells and can thus potentiate vascular disease development. Our data suggest that one of the major changes precipitating these effects is the activation of calpain. However, studying the relevance of these proteases in a human population is hampered by the fact that specific inhibitors are not available for human studies. Therefore, in the present study, we made use of a previously observed phenomenon: that PPARγ agonist therapy attenuates platelet Ca^{2+} levels and calpain activity.[12] Our approach also meant that any positively regulated proteins could either be calpain substrates or proteins directly regulated by PPARγ. Interestingly, although we did detect one such protein (GPD2), a high percentage of the proteins sampled from the gels were previously characterized calpain substrates.

The first novel calpain substrate identified was septin-5 (also known as CDCrel-1 or PNUT-like), a SNARE-interacting protein previously identified as a Parkin substrate and implicated in the regulation of dopaminergic neurons.[27,28] Interestingly, a neuron defect has been difficult to document in septin-$5^{-/-}$ mice, but platelets lacking the protein demonstrate enhanced aggregation and release stored granule products in response to stimuli that are under the threshold for normal platelets.[15] Septin-5 has been localized to membrane areas surrounding platelet α-granules and binds syntaxin 4 to prevent rather than promote secretion.[29] To date, it has been presumed that the phosphorylation of septin-5 in response to platelet agonists dissolves its association with syntaxin to promote granule product release[29]; however, our data suggest that this can also be achieved by the limited proteolysis of the protein by calpain. This implies that the loss of septin-5 function would result in enhanced secretion of platelet α-granule contents in the absence of overt platelet activation, which is exactly what was observed after calpain activation. More recently, different subpopulations of

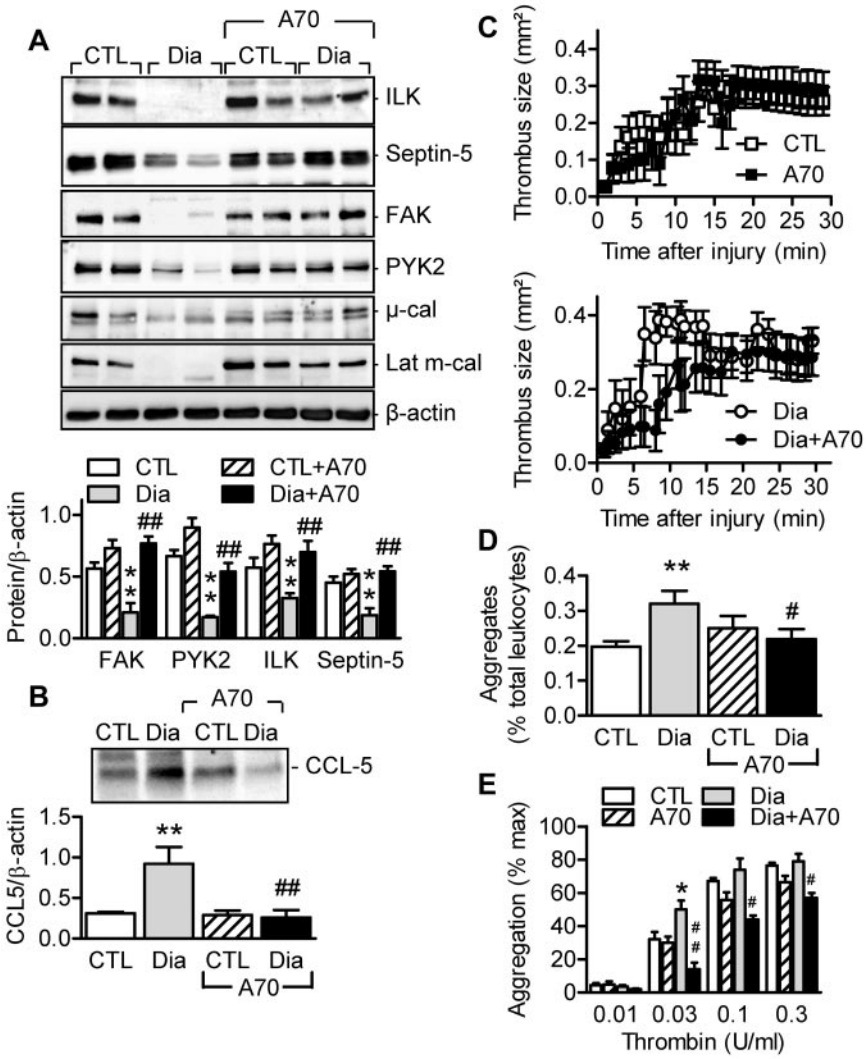

Figure 6. Reversal of the diabetes-associated calpain overactivation by in vivo calpain inhibition. (A) ILK, septin-5, FAK, and PYK2 levels in platelets from healthy (CTL) and streptozotocin-induced diabetic mice (Dia) treated with vehicle or the calpain inhibitor A-705253 (A70). (B) CCL5 in microparticles isolated from the plasma of healthy (CTL) or diabetic (Dia) mice treated with vehicle or A-705253. (C) Effect of in vivo A-705253 treatment on thrombus size after $FeCl_3$-induced injury of carotid arteries from healthy (top panel) and diabetic (bottom panel) mice. (D) Number of circulating platelet-leukocyte aggregates in healthy (CTL) and diabetic (Dia) mice treated with vehicle or A-705253. (E) Aggregation of platelets from healthy and diabetic mice treated with vehicle or A-705253. The graphs summarize data obtained in platelets from 6-9 animals per group. $^{*}P < .05$; $^{**}P < .01$ versus CTL; $\#P < .05$; $\#\#P < .01$ versus vehicle-treated diabetic mice.

α-granules have been proposed to exist,[30,31] and it will be interesting to determine whether calpain activation selectively results in the release of different α-granule subtypes.

In the present study, we focused on CCL5 as a marker of α-granule release, largely because of its described role in promoting the development of atherosclerosis.[16,26] We found that calpain activation promoted the release of CCL5 and that the protein itself is a calpain substrate. The finding that μ-calpain was also secreted from thrombin-stimulated platelets, although initially unexpected, was consistent with our own finding that plasma calpain activity is much higher in samples from diabetic patients than from healthy subjects. It also fits well with a recent report that identified calpain in the platelet secretome.[17] We also observed that the in vitro incubation of CCL5 with calpain resulted in the modification of CCL5 and the generation of a truncated variant (CCL5 3-21) that was more chemotactic for monocytes than the full-length protein. More than 19 variants of CCL5 are known to exist,[32] and proteases such as dipeptidyl peptidase IV and cathepsin G can generate 3-68 and 4-68 variants of CCL5.[33,34] Although the clinical significance of these variants is unclear, higher plasma levels of CCL5 (3-68) have been reported in patients with type 2 diabetes.[32] However, the latter peptide was reported to show reduced rather than enhanced activity toward cells expressing the recombinant CCR5 receptor.[33] This was not unexpected, because the *N*-terminus of many chemokines plays a critical role in the recognition and functional activation of cognate receptors. Given that the variant generated by calpain (3-21) enhanced monocyte adherence, it seems that calpain-mediated modifications of the C-terminus of CCL5 may more than compensate for the lower activity resulting from N-terminal truncation. It is unclear at the moment whether other platelet-derived products may be modified by extracellular calpain, but not all chemokines are calpain substrates, because MCP-1 could not be cleaved by calpain in an in vitro assay.

The second novel calpain substrate we focused on was ILK, which was first identified using a yeast 2-hybrid screen for β1-integrin–binding partners.[35] ILK is part of the focal adhesion complex together with PINCH and Parvin,[18] but even though kinase activity has been shown consistently with a recombinant protein,[20,35] whether it acts as a kinase in vivo has proven controversial.[36-38] Despite the controversy, a dual role for ILK in regulating integrin function and α-granule secretion can be extrapolated from studies in platelets from ILK-deficient mice. The latter demonstrate reduced aggregation, fibrinogen binding, and arterial thrombus formation, as well as a selective defect in α-granule but not dense-granule secretion.[39] This phenotype fits well with that of the diabetic platelet. In addition, the results of the present study indicate that ILK is inactive when associated with PINCH and that μ-calpain initiates their dissociation and the subsequent phosphorylation of the ILK downstream target, Akt. A similar mechanism of action was recently proposed in a study looking at heart failure in

zebrafish induced by the down-regulation of PINCH, which led to instability of ILK and the loss of Akt activity.[40] Whereas our data suggest that μ-calpain is required for the activation of ILK, it seems that the activation of m-calpain results in the degradation of the kinase and prevents Akt phosphorylation.

Given the role of the IPP complex in the regulation of integrin signaling and the fact that the proteolysis of focal adhesion proteins such as talin, paxillin, FAK, and PYK2 is known to regulate focal adhesion dynamics and cell migration,[22,23] it was logical to look at the consequences of calpain activation on platelet adhesion and spreading. We found that μ-calpain activation, which was also required for the activation of ILK, seems to regulate platelet adhesion (at least on fibronectin), whereas m- rather than μ-calpain regulates platelet spreading. The latter could be concluded only by comparing responses in platelets from μ-cal$^{fl/fl}$ and PF4-μ-cal$^{-/-}$ mice, because none of the currently available calpain inhibitors can differentiate between the μ- and m-calpain isoforms. Although the full spectrum of platelet kinases targeted by calpains remains to be elucidated, our data suggest that in vitro calpain activation and that associated with the development of diabetes must be linked with major changes in different intracellular signaling cascades. Indeed, ILK, PYK2, and FAK levels were almost undetectable in platelets from healthy subjects or mice after calpain activation in vitro or in diabetic platelets. However, normal levels of the kinases were observed in platelets from patients treated with a PPARγ agonist and diabetic animals treated with a calpain inhibitor.

It is well accepted that platelets contribute actively to the diabetes-associated accelerated development of atherothrombosis and enhanced platelet reactivity may account for the refractory response of diabetic patients to conventional antiplatelet therapy. The findings that calpain activity is elevated in platelets from diabetic subjects and that a calpain inhibitor reversed the diabetes-induced hyperactivation of platelets in mice suggest that Ca^{2+}-activated proteases may be a promising therapeutic target for a better management of diabetes-associated platelet and vascular complications. Calpain inhibition may also underlie platelet activation in other conditions, because many of the proteins identified as calpain substrates in diabetic humans and mice (including ILK) were also reported to be altered in platelets from patients with acute coronary syndromes.[41,42]

Although in the present study, we found no significant effects on platelet number or function in otherwise healthy mice after 12 days of treatment, other studies indicate that the long-term treatment with A-705253 is well tolerated and can protect against retinal damage[43] and penile nitrergic nerve and dysfunction in diabetic mice.[44] Other calpain inhibitors attenuate angiotensin II–induced abdominal aortic aneurysms and atherosclerosis in LDL receptor–deficient mice[45] and angiotensin II–induced endothelial dysfunction in rats and mice.[46] The results of the present study, together with the studies showing a beneficial effect of calpain inhibition in vascular disease, highlight the potential of calpain inhibition for the treatment of the vascular complications of type 2 diabetes. However, future efforts should focus on the development of compounds devoid of the problems of calpain isoform selectivity and specificity versus other proteases,[47] which have hampered the progression of calpain inhibitors into clinical trials.

Acknowledgments

The authors thank Isabel Winter, Ingrid Kempter, and Katharina Engel-Herbig for technical assistance and Rory R. Koenen and Christian Weber (Ludwig Maximilians University, Munich, Germany) for help with CCL5 staining in carotid arteries.

This study was supported by the Deutsche Forschungsgemeinschaft (SFB 815/A16 and Z1 and the Exzellenzcluster 147 Cardio-Pulmonary System) and by the European Vascular Genomic Network, a network of excellence supported by the European Community's Sixth Framework Program (contract number LSHM-CT-2003-503254). A.E. was supported by a German Egyptian Research Long-term Scholarship funded by the Egyptian Ministry of Higher Education and Scientific Research and the German Academic Exchange Service. M.M. is a Senior Fellow of the British Heart Foundation.

Authorship

Contribution: V.R. codesigned the study, performed the experiments, and interpreted the results; J.I. and A.E. performed the experiments with human and murine platelets; F.P. performed the pioglitazone study and prepared the platelet samples; T.F. generated the PF4-μ-cal$^{-/-}$ mice; X.Y. and M.M. performed the differential in gel electrophoresis analysis of diabetic samples; K.B. provided the blood samples from characterized diabetic patients; H.H. performed the MS analysis of CCL5; and I.F. designed the study and wrote the manuscript.

Conflict-of-interest disclosure: The authors declare no competing financial interests.

Correspondence: Ingrid Fleming, PhD, Institute for Vascular Signalling, Centre for Molecular Medicine, Goethe University, Theodor-Stern-Kai 7, D-60590 Frankfurt am Main, Germany; e-mail: fleming@em.uni-frankfurt.de.

References

1. Sorimachi H, Hata S, Ono Y. Impact of genetic insights into calpain biology. *J Biochem*. 2011; 150(1):23-37.
2. Croall D, Ersfeld K. The calpains: modular designs and functional diversity. *Genome Biol*. 2007;8(6):218.
3. Suzuki K, Hata S, Kawabata Y, Sorimachi H. Structure, activation, and biology of calpain. *Diabetes*. 2004;53(90001):S12-S18.
4. Hood JL, Brooks WH, Roszman TL. Subcellular mobility of the calpain/calpastatin network: an organelle transient. *BioEssays*. 2006;28(8):850-859.
5. Liu T, Schneider RA, Hoyt DG. Calpastatin is regulated by protein never in mitosis gene A interacting-1 (PIN1) in endothelial cells. *Biochem Biophys Res Commun*. 2011;414(3):581-586.
6. Shao H, Chou J, Baty CJ, et al. Spatial localization of m-calpain to the plasma Membrane by phosphoinositide biphosphate binding during epidermal growth factor receptor-mediated activation. *Mol Cell Biol*. 2006;26(14):5481-5496.
7. Beltran L, Chaussade C, Vanhaesebroeck B, Cutillas PR. Calpain interacts with class IA phosphoinositide 3-kinases regulating their stability and signaling activity. *Proc Natl Acad Sci U S A*. 2011;108(39):16217-16222.
8. Dutt P, Croall D, Arthur JS, et al. m-Calpain is required for preimplantation embryonic development in mice. *BMC Dev Biol*. 2006;6(1):3.
9. Takano J, Mihira N, Fujioka R, et al. Vital role of the calpain-calpastatin system for placental-integrity-dependent embryonic survival. *Mol Cell Biol*. 2011;31(19):4097-4106.
10. Azam M, Andrabi SS, Sahr KE, et al. Disruption of the mouse mu-calpain gene reveals an essential role in platelet function. *Mol Cell Biol*. 2001; 21(6):2213-2220.
11. Kuchay SM, Kim N, Grunz EA, Fay WP, Chishti AH. Double knockouts reveal that protein tyrosine phosphatase 1B is a physiological target of calpain-1 in platelets. *Mol Cell Biol*. 2007; 27(17):6038-6052.
12. Randriamboavonjy V, Pistrosch F, Bolck B, et al. Platelet sarcoplasmic endoplasmic reticulum Ca2+-ATPase and mu-calpain activity are altered in type 2 diabetes mellitus and restored by rosiglitazone. *Circulation*. 2008;117(1):52-60.
13. Kuchay SM, Chishti AH. Calpain-mediated regulation of platelet signaling pathways. *Curr Opin Hematol*. 2007;14(3):249-254.

14. Bogacka I, Xie H, Bray GA, Smith SR. The effect of pioglitazone on peroxisome proliferator-activated receptor-gamma target genes related to lipid storage in vivo. *Diabetes Care*. 2004;27(7):1660-1667.
15. Dent J, Kato K, Peng XR, et al. A prototypic platelet septin and its participation in secretion. *Proc Natl Acad Sci U S A*. 2002;99(5):3064-3069.
16. Schober A, Zernecke A. Chemokines in vascular remodeling. *Thromb Haemost*. 2007;97(5):730-737.
17. Fong KP, Barry C, Tran AN, et al. Deciphering the human platelet sheddome. *Blood*. 2011;117(1):e15-e26.
18. Legate KR, Montanez E, Kudlacek O, Fassler R. ILK, PINCH and Parvin: the tIPP of integrin signalling. *Nat Rev Mol Cell Biol*. 2006;7(1):20-31.
19. Persad S, Attwell S, Gray V, et al. Inhibition of integrin-linked kinase (ILK) suppresses activation of protein kinase B/Akt and induces cell cycle arrest and apoptosis of PTEN-mutant prostate cancer cells. *Proc Natl Acad Sci U S A*. 2000;97(7):3207-3212.
20. Persad S, Attwell S, Gray V, et al. Regulation of protein kinase B/Akt-serine 473 phosphorylation by integrin-linked kinase: critical roles for kinase activity and amino acids arginine 211 and serine 343. *J Biol Chem*. 2001;276(29):27462-27469.
21. Zhang Y, Chen K, Tu Y, et al. Assembly of the PINCH-ILK-CH-ILKBP complex precedes and is essential for localization of each component to cell-matrix adhesion sites. *J Cell Sci*. 2002;115(Pt 24):4777-4786.
22. Franco SJ, Rodgers MA, Perrin BJ, et al. Calpain-mediated proteolysis of talin regulates adhesion dynamics. *Nat Cell Biol*. 2004;6(10):977-983.
23. Chan KT, Bennin DA, Huttenlocher A. Regulation of adhesion dynamics by calpain-mediated proteolysis of focal adhesion kinase (FAK). *J Biol Chem*. 2010;285(15):11418-11426.
24. Lubisch W, Beckenbach E, Bopp S, et al. Benzoylalanine-derived ketoamides carrying vinylbenzyl amino residues: discovery of potent water-soluble calpain inhibitors with oral bioavailability. *J Med Chem*. 2003;46(12):2404-2412.
25. Massberg S, Konrad I, Schurzinger K, et al. Platelets secrete stromal cell-derived factor 1alpha and recruit bone marrow-derived progenitor cells to arterial thrombi in vivo. *J Exp Med*. 2006;203(5):1221-1233.
26. Koenen RR, von Hundelshausen P, Nesmelova IV, et al. Disrupting functional interactions between platelet chemokines inhibits atherosclerosis in hyperlipidemic mice. *Nat Med*. 2009;15(1):97-103.
27. Beites CL, Campbell KA, Trimble WS. The septin Sept5/CDCrel-1 competes with alpha-SNAP for binding to the SNARE complex. *Biochem J*. 2005;385(2):347-353.
28. Son JH, Kawamata H, Yoo MS, et al. Neurotoxicity and behavioral deficits associated with Septin-5 accumulation in dopaminergic neurons. *J Neurochem*. 2005;94(4):1040-1053.
29. Beites CL, Xie H, Bowser R, Trimble WS. The septin CDCrel-1 binds syntaxin and inhibits exocytosis. *Nat Neurosci*. 1999;2(5):434-439.
30. Italiano JE, Jr., Richardson JL, Patel-Hett S, et al. Angiogenesis is regulated by a novel mechanism: pro- and antiangiogenic proteins are organized into separate platelet alpha granules and differentially released. *Blood*. 2008;111(3):1227-1233.
31. Battinelli EM, Markens BA, Italiano JE. Release of angiogenesis regulatory proteins from platelet alpha granules: modulation of physiological and pathological angiogenesis. *Blood*. 2011;118(5):1359-1369.
32. Oran PE, Sherma ND, Borges CR, Jarvis JW, Nelson RW. Intrapersonal and populational heterogeneity of the chemokine RANTES. *Clin Chem*. 2010;56(9):1432-1441.
33. Oravecz T, Pall M, Roderiquez G, et al. Regulation of the receptor specificity and function of the chemokine RANTES (regulated on activation, normal T cell expressed and secreted) by dipeptidyl peptidase IV (CD26)-mediated cleavage. *J Exp Med*. 1997;186(11):1865-1872.
34. Lim JK, Lu W, Hartley O, DeVico AL. N-terminal proteolytic processing by cathepsin G converts RANTES/CCL5 and related analogs into a truncated 4-68 variant. *J Leukoc Biol*. 2006;80(6):1395-1404.
35. Hannigan GE, Leung-Hagesteijn C, Fitz-Gibbon L, et al. Regulation of cell adhesion and anchorage-dependent growth by a new beta$_1$-integrin-linked protein kinase. *Nature*. 1996;379:91-96.
36. Wickström SA, Lange A, Montanez E, Fassler R. The ILK/PINCH/Parvin complex: the kinase is dead, long live the pseudokinase! *EMBO J*. 2010;29(2):281-291.
37. Fukuda K, Knight JDR, Piszczek G, Kothary R, Qin J. Biochemical, proteomic, structural, and thermodynamic characterizations of integrin-linked kinase (ILK). *J Biol Chem*. 2011;286(24):21886-21895.
38. Hannigan GE, McDonald PC, Walsh MP, Dedhar S. Integrin-linked kinase: Not so 'pseudo' after all. *Oncogene*. 2011;30:4375-4385.
39. Tucker KL, Sage T, Stevens JM, et al. A dual role for integrin-linked kinase in platelets: regulating integrin function and alpha-granule secretion. *Blood*. 2008;112(12):4523-4531.
40. Meder B, Huttner IG, Sedaghat-Hamedani F, et al. PINCH proteins regulate cardiac contractility by modulating integrin linked kinase-protein kinase B signaling. *Mol Cell Biol*. 2011;31:3424-3435.
41. Parguiña AF, Grigorian-Shamajian L, Agra RM, et al. Proteins involved in platelet signaling are differentially regulated in acute coronary syndrome: a proteomic study. *PLoS One*. 2010;5(10):e13404.
42. Parguiña AF, Grigorian-Shamagian L, Agra RM, et al. Variations in platelet proteins associated with ST-elevation myocardial infarction: novel clues on pathways underlying platelet activation in acute coronary syndromes. *Arterioscler Thromb Vasc Biol*. 2011;31(12):2957-2964.
43. Shimazawa M, Suemori S, Inokuchi Y, et al. A novel calpain inhibitor, ((1S)-1-((((1S)-1-Benzyl-3-cyclopropylamino-2,3-di-oxopropyl) mino)carbony l)-3-methylbutyl)carbamic acid 5-methoxy-3-oxapentyl ester (SNJ-1945), reduces murine retinal cell death in vitro and in vivo. *J Pharmacol Exp Ther*. 2010;332(2):380-387.
44. Nangle MR, Cotter MA, Cameron NE. The calpain inhibitor, A-705253, corrects penile nitrergic nerve dysfunction in diabetic mice. *Eur J Pharmacol*. 2006;538(1-3):148-153.
45. Subramanian V, Uchida HA, Ijaz T, et al. Calpain inhibition attenuates angiotensin II-induced abdominal aortic aneurysms and atherosclerosis in LDL receptor deficient mice. *J Cardiovasc Pharmacol*. 2012;59(1):66-76.
46. Scalia R, Gong Y, Berzins B, et al. A novel role for calpain in the endothelial dysfunction induced by activation of angiotensin II type 1 receptor signaling / novelty and significance. *Circ Res*. 2011;108(9):1102-1111.
47. Donkor IO. Calpain inhibitors: a survey of compounds reported in the patent and scientific literature. *Expert Opin Ther Pat*. 2011;21(5):601-636.

CALPAIN INHIBITION STABILIZES THE PLATELET PROTEOME AND REACTIVITY IN DIABETES

Supplementary materials and methods

Reagents

Cell culture media were purchased from Gibco (Invitrogen; Darmstadt, Germany). Calpeptin was from Calbiochem (Darmstadt, Germany), type I Collagen and fibronectin were from BD transduction laboratories (Heidelberg, Germany). Thrombin was from Hemochrom Diagnostica (Essen, Germany), The calpain inhibitor N-(1-benzyl-2-carbamoyl-2-oxoethyl)-2-[E-2-(4-diethyl-aminomethylphenyl)ethen-1-yl]benzamide (A-705253) was provided by Abbott GmbH & Co KG (Ludwigshafen, Germany). The anti-Akt and anti-Ser734-Akt antibodies were from Cell Signaling (New England Biolabs, Frankfurt, Germany), the anti-FAK, the anti-α-parvin, anti-septin-5, anti-ILK and the anti-syntaxin-4 antibodies were from Abcam (Cambridge, UK), the anti-CCL5 was from Molecular Probes (Invitrogen; Darmstadt, Germany), the anti-PINCH and anti-PYK2 antibodies were from BD transduction laboratories (Heidelberg, Germany); anti-PECAM1 was from Dako (Glostrup, Denmark). All other compounds were from Sigma-Aldrich (Steinheim, Germany).

Pioglitazone study population

A total of 13 patients (5 women, 8 men; mean age, 47±5.4 years; age range, 30 to 70 years) with type 2 diabetes mellitus were used in this study. Patients were treated with either pioglitazone 30 mg/day (Actos®, Takeda; Aachen, Germany) or placebo each for 12 weeks in a cross sectional design. There was a 4 week washout period between the different treatments. The study protocol was approved by the ethics committee of the Technical University of Dresden (No. EK 233112006), and all of the participants gave written informed consent. Nondiabetic, age-matched subjects (7 women, 8 men; mean age, 40.25±6.5 years; age range, 23 to 50 years; HbA_{1c}, 5.2±0.6%; fasting plasma glucose, 5.1±0.2 mmol/L) who had not taken any medication known to interfere with platelet aggregation for at least 10 days before the experiment served as the control group.

Diabetic population

A total of 30 patients (16 women, 14 men; mean age, 47±5.4 years; age range, 30 to 70 years) with type 2 diabetes mellitus attending the clinic for routine control visits were included in the study. Hemoglobin (Hb) A_{1c},over 7.4% and fasting plasma glucose, 8.2±0.7 mmol/L. All patients were treated with insulin alone or in combination with metformin. Nondiabetic, age-matched subjects (12 women, 18 men; mean age, 42.4±4.5 years; age range, 25 to 65 years; HbA_{1c}, 5.2±0.6%; fasting plasma glucose, 5.1±0.2 mmol/L) who had not taken any medication known to interfere with platelet aggregation for at least 10 days before the experiment served as the control group. The study protocol was approved by the ethics committee of the Goethe University Hospital (No. E 61/09 geschäfts Nr 86/09) and all of the participants gave written informed consent.

Proteomic analysis

Platelet extracts were prepared using a lysis buffer (8M urea, 4% w/v CHAPS, 30mM Tris-Cl, pH 8.5) compatible with DIGE labeling (GE healthcare). After centrifugation at 13,000g for 10 minutes, the supernatant containing soluble proteins was harvested and the protein concentration was determined using a modification of the method described by Bradford. The fluorescence dye labeling reaction was carried out at a dye/protein ratio of 200pmol/50µg. After incubation on ice for 30 minutes, the labelling reaction was stopped by scavenging non-bound dyes with 10mM lysine (L8662, Sigma) for 15 minutes. For two-dimensional gel electrophoresis, samples were mixed with 2x buffer (8M urea, 4% w/v CHAPS, 2% w/v DTT, 2% v/v Pharmalytes 3-10 for IEF), 50µg per sample were diluted in rehydration solution (8M urea, 0.5% w/v CHAPS, 0.2% w/v DTT, and 0.2% v/v Pharmalyte pH 3-10) and loaded on IPG strips (18cm, pH 3-10, nonlinear, GE healthcare). After rehydration overnight, strips

were focused at 0.05 mA/IPG strip for 28 kVh at 20°C (IPGphor, GE healthcare). Once IEF was complete the strips were equilibrated in 6M urea containing 30% v/v glycerol, 2% w/v SDS and 0.01% w/v Bromophenol blue, with addition of 1% w/v DTT for 15 minutes, followed by the same buffer without DTT, but with the addition of 4.8% w/v iodoacetamide for 15 minutes. SDS-PAGE was performed using 12% T (total acrylamide concentration), 2.6% C (degree of cross-linking) polyacrylamide gels without a stacking gel, using the Ettan DALT system (GE healthcare). The second dimension was terminated when the Bromophenol blue dye front had migrated off the lower end to the gels. After electrophoresis, fluorescence images were acquired using the Ettan DIGE imager (GE healthcare). Finally, gels were fixed overnight in methanol: acetic acid: water solution (4:1:5 v/v/v). Protein profiles were visualized by silver staining using the Plus one silver staining kit (GE healthcare), with slight modifications,[1] to ensure compatibility with subsequent mass spectrometry analysis. For documentation, silver-stained gels were scanned in transmission scan mode using a calibrated scanner (GS-800, Bio-Rad). DIGE gels were analyzed using the Decyder software (Version 7.0, GE healthcare). All 2-DE gels were of high quality in terms of resolution as well as consistency in spot patterns. Spots exhibiting a statistical difference (fold change >1.2, $p<0.05$) were excised for identification. A detailed methodology is available at http://www.vascular-proteomics.com.

Tandem Mass Spectrometry

In-gel digestion with trypsin was performed according to published methods[2] modified for use with an Investigator ProGest (Genomic Solutions) robotic digestion system. Following enzymatic degradation, samples were separated by liquid chromatography on a reverse-phase column (C18 PepMap100, 3 µm, 100Å, 25 cm, Dionex) and applied to a LTQ Orbitrap XL mass spectrometer (Thermo Scientific). Spectra were collected from the mass analyzer using full ion scan mode over the m/z range 450-1600. Six dependent MS/MS scans were performed on each ion using dynamic exclusion. Database searches were performed using the TurboSEQUEST software (Bioworks Browser version 3.3.1, Thermo Fisher) against human database (20333 protein entries, UniProt KB Release 14.6, 16-Dec-2008) and the following filters were applied (Scaffold software, version 2.6, Proteome Software): peptide probability > 95%, protein probability >99.9%, minimum no. of peptides per protein >=2.

Calpain cleavage of CCL5 (RANTES)

Recombinant CCL5 (Sigma-Aldrich) was incubated with recombinant calpain (Sigma-Aldrich; 1U, 30°C, 30 minutes). Calpain was activated by adding cysteine (5 mmol/L) and Ca^{2+} (5 mmol/L) to the reaction buffer.

MS analysis of CCL5

CCL5 and calpain-treated CCL5 samples were separated by SDS-PAGE and the corresponding area cut into slices. After reduction and carbamidomethylation gel pieces were digested overnight with MS grade trypsin (Promega), the extracted peptides were then lyophilized and resuspended in 5% acetonitrile/0.5% formic acid. The MS analysis of tryptic digested proteins was performed by nano-LC-MS/MS and CID fragmentation on an LTQ-Orbitrap mass spectrometer. Mass spectra were analyzed by Mascot Server 2.2 by matching them against the *Homo sapiens* Uniprot protein database. The following Mascot search parameters were used: maximum of one missed cleavage, cysteine carbamidomethylation, methionine oxidation and mass tolerance for MS scans of 8 ppm and 0.8 Da for MS/MS, respectively. The Mascot searches were performed in a first round using the error-tolerant search option and after the cleavage sites in CCL5 had been identified, the sequences of CCL5 in the database were shortened according to the identified cleavage site and Mascot searches repeated without the error-tolerant search option. Only peptides with individual ions scores indicating identity or extensive homology; ($P<0.05$) were taken into account.

Animals

C57BL/6 mice (6-8 weeks old) were from Charles River (Sulzfeld, Germany). Floxed µ-calpain$^{-/-}$ mice were generated by TaconicArtemis GmbH (Cologne, Germany) and bred with

animals expressing the Cre-deleter under the control of the PF4 promoter (The Jackson Laboratory, Bar Harbor, Maine, USA) to generate mice lacking μ-calpain in platelets.

Briefly, mice were generated using C57BL/6 embryonic stem cells for gene targeting. Positive selection cassettes flanked by FRT/F3 sites were deleted by crossing with a ubiquitously expressing FLP1 recombinase strain (**Figure I**). Excision after Cre recombination was confirmed by PCR with primers to detect a floxed portion of the construct 5'-TCT ACG TAC AGG GTT CCA AGC-3', 5'-CCA CGA GAG GGT GT TAG ACC-3' with 213 bp product lengths for the wild-type alleles, 397 bp for the conditional alleles (loxP and F3) and by PCR with primers to detect the portion of the targeting construct that remains in the genome: 5'-GCT TAG AGG CTA ACA GCT AGA CC-3' and 5'-GGT CTAA CAC CCT CTC GTG G-3' (300 bp), product specificity were demonstrated by *HindIII* digestion resulting in a 181 and 119 bp fragment. Genomic DNA from tail samples were used for the PCR genotyping with the following parameters: 95°C for 5 minutes, followed by 35 cycles, at 95°C for 30 seconds, 60°C for 30 seconds, 72°C for 30 seconds and 72°C for 10 minutes. For PF4-cre detection the primers used were: 5´-CCC ATA CAG CAC ACC TTT TG-3´ and 5´-TGC ACA GTC AGC AGG TT-3´ with the following parameters: 94°C for 5 minutes, followed by 30 cycles, at 95°C for 30 seconds, 60°C for 30 seconds, 72°C for 30 seconds and 72°C for 2 minutes. Gt(ROSA)26Sor$^{tm16(Cre)Arte}$ (TaconicArtemis) was detected with the following primers 5´-ACG ACC AAG TGA CAG CAA TG and CTC GAC CAG TTT AGT TAC CC.

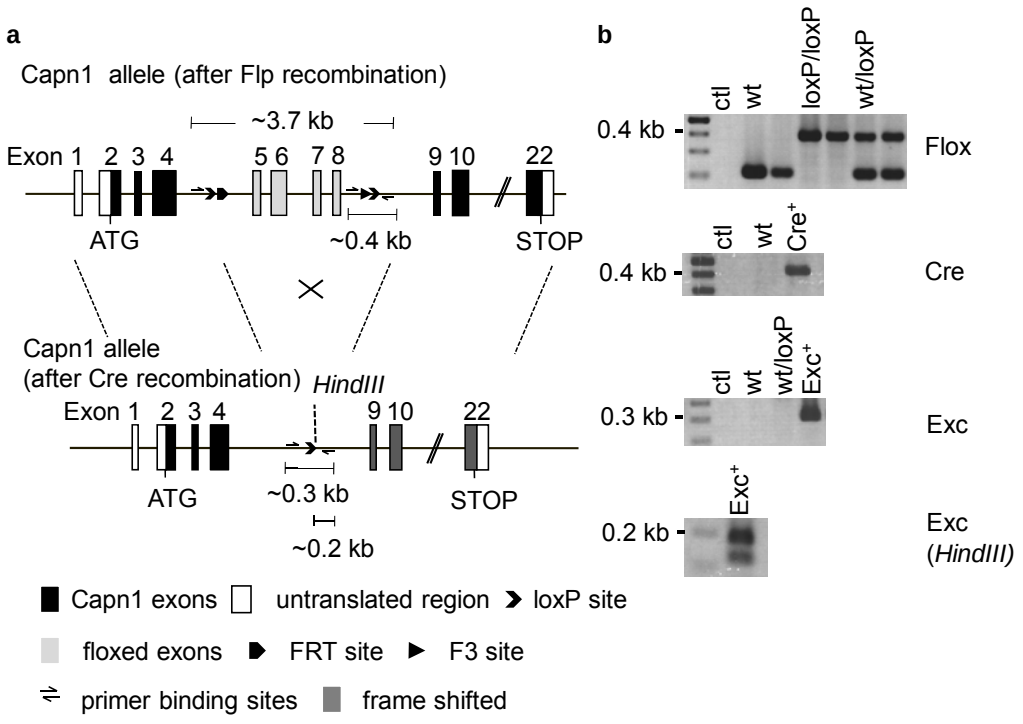

Figure I. Platelet-specific μ-calpain$^{-/-}$ mouse. (**a**) Schematic depiction of the targeted Capn1 locus after Flp/Cre recombination, including primer binding sites for genotyping. (**b**) PCR analysis showing the detection of the floxed locus (Flox) for the WT/loxP alleles (213 bp, 397bp respectively), and detection of excision (Exc, 300 bp) after Cre (Gt(ROSA)26Sor$^{tm16(Cre)Arte}$; 0.4 kb) recombination. The PCR product detecting excision was verified via HindIII digestion (181 and 119 bp).

Diabetes induction

Diabetes was induced with a single intraperitoneal injection of streptozotocin (150 mg/kg) and animals were considered diabetic when fasting plasma glucose was over 250 mg/dl. In

some experiments animals were treated by oral gavage with the calpain inhibitor A-705253 (30 mg/kg/day) for 12 days after 12 weeks untreated diabetes.

Platelet isolation

Human platelets: Platelets were obtained by centrifugation (900*g*, 7 minutes) of platelet-rich plasma, as described.[3] The resulting pellet was washed in Ca^{2+}-free HEPES buffer (mmol/L: NaCl, 136; KCl, 2.6; $MgCl_2$, 0.93; NaH_2PO_4, 3.26; glucose, 5.5; HEPES, 3.7; pH 7.4 at 37°C). Platelet pellets were snap frozen with liquid nitrogen and stored at -80°C until use for Western blot or resuspended in HEPES buffer to a density of $4x10^8$ platelets/mL for the measurement of intracellular Ca^{2+} or platelet aggregation as described.[4]

Murine platelets: Mice were anesthetized with isoflurane and blood was collected via cardiac puncture into a syringe containing 10% acidic citrate dextrose (120 mmol/L sodium citrate, 110 mmol/L glucose, 80 mmol/L citric acid) as anticoagulant. Platelets were prepared from whole blood by differential centrifugation and resuspended in Ca^{2+}-free HEPES buffer to a density of $8x10^8$ platelets/mL. $[Ca^{2+}]_i$ was determined by measuring changes in fura-2 fluorescence as described.[4]

***In vitro* calpain substrate determination**

μ-Calpain was activated by incubation of washed platelets with 5 mmol/L $CaCl_2$ for 30 minutes as described[5] and m-calpain was activated by $CaCl_2$ (5 mmol/L) and ionomycin (1 μmol/l).

Calpain activity assay

Calpain activity was assessed by monitoring the formation of the fluorescent metabolite 7-amino-4-methylcoumarin (AMC) from N-succinyl-Leu-Leu-Val-Tyr7-amido-4-methylcoumarin.

ILK activity assay

ILK was co-immunoprecipitated with PINCH from Triton X-100-soluble platelet lysate. The immunoprecipitate was treated with solvent, μ-calpain or m-calpain (1U/mL for 30 minutes at 30°C) in order to induce ILK cleavage. The complex was then added to platelet lysates (obtained after 3 cycles of freezing and thawing) as a source of Akt. Reactions were stopped after 10 minutes by adding SDS sample buffer.

Immunoblotting

Washed human or murine platelets were solubilized in Triton X-100 lysis buffer and Triton X-100 soluble proteins were separated by SDS-PAGE and subjected to Western blotting and visualized by enhanced chemiluminescence using a commercially available kit (Amersham, Freiburg, Germany), as described.[6]

Platelet-derived microparticles

Microparticles were isolated by centrifugation of platelet poor plasma (40000g, 4°C, 45 minutes). After washing, microparticles were resuspended in platelet HEPES buffer and labeled with either a FITC-conjugated anti-human CD61 antibody (BD Pharmingen) or a FITC-conjugated IgG1κ isotype control (BD Pharmingen). The suspension was washed, resuspended in PBS and analyzed in a FACScan flow cytometer using a CellQuest software (Becton Dickinson, CA). Human platelet-derived microparticles were 62.8±7.9% of total circulating microparticles in healthy individuals.

Platelet aggregation

Aggregation of washed human or murine platelets ($4x10^8$ platelets/mL) was measured as described[4] using an 8-channel aggregometer (PAP8, Mölab, Germany).

Clot retraction

Platelet-rich plasma (adjusted to $300x10^9$ platelets/mL for human platelets and $5x10^8$ platelets/mL for murine platelets, 300 μL) obtained by centrifugation of whole blood at 250*g* for 10 minutes, was stimulated with thrombin (0.3 U/mL for human and 1U/mL for murine) in

the presence of $CaCl_2$ (20 mmol/L) and 10 µL erythrocytes to enhance the contrast of the clot. The clots were allowed to retract for up to 3 hours at 37°C and were photographed at different time points. The extent of retraction was quantified using TINA20 software (Raytest GmbH, Straubenhardt, Germany).

Thrombus formation in a $FeCl_3$-induced carotid artery model

To assess thrombus formation *in vivo*, mice were anesthetized by intraperitoneal injection of ketamine and xylazine and placed on a heated mat. The fluorescent dye 3,3'-dihexyloxacarbocyanine iodide ($DIOC_6$; Ivitrogen, Darmstadt, Germany) was injected into the jugular vein (5 µL of a 100 µmol/L solution/g body weight) to allow visualization of the thrombus. Thereafter, a segment of the right carotid artery was exposed and injury was induced by the topical application of $FeCl_3$ for 2 minutes (Whatmann paper 1 mm^2 soaked with 0.2 µL of 10% $FeCl_3$) as described.[4] The artery was then rinsed with saline and thrombus formation was monitored for 30 minutes by placing the carotid artery under a fluorescence microscope equipped with a camera (AxioScope, Carl Zeiss, Jena, Germany). Fluorescent images were acquired sequentially (1 image/second) and thrombus size was quantified using AxioVision 4.7 imaging software (Carl Zeiss).

Platelet adhesion and spreading assays

Static adhesion assays were performed as described.[7] Washed human or murine platelets were stimulated or not with 5 mmol/L $CaCl_2$ in the absence or in the presence of the calpain inhibitor calpeptin. Platelet suspensions ($5x10^4$ platelets/µL) were seeded on glass slides (µ-Slide 8 well, ibidi, Martinsried, Germany), coated with fibronectin (100 µg/mL) and incubated at 37°C for 15 minutes for human platelets and 60 minutes for murine platelets. Non adherent platelets were washed out and adherent and spread platelets were fixed. Images were captured by a AxioCam MRm on a Cell Observer microscope (Zeiss, Jena, Germany) and analyzed using the imaging software AxioVision 4.8 (Zeiss, Jena, Germany).

Platelet-derived products

Washed human platelets were stimulated or not with $CaCl_2$ (5 mmol/L) for 30 minutes and then centrifuged (800g, 5 minutes, 37°C). Platelets were resuspended in HEPES buffer and stimulated with thrombin (1U/mL) for 10 minutes at 37°C. The platelet suspension was again centrifuged (800g, 5 minutes, 37°C) and the supernatant was collected and directly placed on ice. Supernatant was ultracentrifuged (50.000g/1h/4°C) in order to remove contaminating microparticle and was either placed on ice for further analysis or stored at -80°C until further use. Transforming growth factor (TGF)-β and CCL5 in the releasate were quantified using commercially available ELISAs (R&D systems, Wiesbaden, Germany) according to the manufacturer's instructions. The serotonin ELISA was from IBL (Hamburg, Germany).

Cell culture

Human umbilical vein endothelial cells were isolated and cultured as described.[8] To assess proliferation, non-confluent cells (passage P1) were stimulated with either vascular endothelial cell growth factor (VEGF; 60ng/mL) or platelet derived products (1:1 dilution with MCDB medium) and maintained in culture. Cells were counted after 48, 72 and 96 hours using the Casy cell counter (Roche, Mannheim, Germany)

THP-1 monocytic cells (ATCC, Wesel, Germany) were cultured in RPMI 1640 containing 100 units/mL penicillin, 100 µg/mL streptomycin and 10% heat inactivated fetal calf serum. THP-1 cell migration was assessed using a modified Transwell chamber system with membrane inserts (8-µm pore size; BD Biosciences, Heidelberg, Germany). Cells were seeded at a density of 100,000 cells/cm^2 in the Transwell inserts and monocyte migration was evaluated by counting the number of cells in the lower wells after 2 hours. Cell migration was assessed in response to fresh culture medium alone, recombinant CCL5, µ-calpain or the µ-calpain-cleaved CCL5.

Immunofluorescence. CCL5 immobilized on the surface of endothelial cells was detected as described.[9] After preincubation with solvent or calpeptin (10 µmol/L, 30 minutes), platelets

were stimulated or not with $CaCl_2$ (5mmol/L, 30 minutes), centrifuged and resuspended in platelet buffer. Platelets were added to endothelial cells under continual shaking (50 rpm, 37°C). After 1 hour the endothelial cells were washed, fixed with 4% paraformaldehyde and blocked with 2% BSA. Samples were then incubated with antibodies against β3-integrin to identify platelets, and anti-CCL5 antibody (VL-1) or its isotype control and corresponding Alexa fluorescent secondary antibodies.

En face staining

Carotid arteries were carefully cleaned of fat and connective tissue. Arteries were opened and labeled *in situ* with anti-CCL5 antibody (R&D Systems, Wiesbaden, Germany), or IgG control coupled to Protein G green fluorescent beads (Spherotech, 1 µm) for 1 hour at 37°C. After washing and fixation with paraformaldehyde (4% v/v in PBS) carotid arteries were mounted on glass slides with fluorescent mounting medium (Dako, Eching, Germany). *En face* images were obtained using a Zeiss LSM-510 meta laser confocal microscope.

Flow cytometry analysis of platelet-leukocyte aggregates

Whole murine blood (100 µL) was incubated with 1 mL erythrocyte lysis buffer to lyse erythrocytes (30 minutes, room temperature). After centrifugation and washing pellets were fixed with formalin (2% vol/vol in PBS) then washed and resuspended in platelet buffer. The suspension was incubated for 15 minutes at room temperature in the dark with a phycoerythrin-conjugated anti-mouse CD45 antibody (BD Biosciences, Heidelberg, Germany) and a FITC-conjugated anti-mouse CD61 antibody (BD Biosciences, Heidelberg, Germany) or matched mouse IgG isotype controls. Samples were then washed and analyzed by flow cytometry (FACS Calibur flow cytometer; BD Biosciences) for single or double-staining.

Statistical analysis

Data are expressed as mean ± SEM and statistical evaluation was performed using Student's t test for unpaired data or one-way analysis of variance (ANOVA) followed by a Bonferroni t test where appropriate using Prism software (GraphPad). Values of $P<0.05$ were considered statistically significant.

References

1. Yan JX, Wait R, Berkelman T et al. A modified silver staining protocol for visualization of proteins compatible with matrix-assisted laser desorption/ionization and electrospray ionization-mass spectrometry. *Electrophoresis* 2000;21(17):3666-3672.
2. Shevchenko A, Wilm M, Vorm O, Mann M. Mass spectrometric sequencing of proteins silver-stained polyacrylamide gels. *Anal Chem* 1996;68(5):850-858.
3. Randriamboavonjy V, Schrader J, Busse R, Fleming I. Insulin induces the release of vasodilator compounds from platelets by a nitric oxide-G kinase-VAMP-3-dependent pathway. *J Exp Med* 2004;199(3):347-356.
4. Randriamboavonjy V, Isaak J, Frömel T et al. AMPK $\alpha 2$ subunit is involved in platelet signaling, clot retraction, and thrombus stability. *Blood* 2010;116(12):2134-2140.
5. Randriamboavonjy V, Pistrosch F, Bolck B et al. Platelet sarcoplasmic endoplasmic reticulum Ca^{2+}-ATPase and µ-calpain activity are altered in type 2 diabetes mellitus and restored by rosiglitazone. *Circulation* 2008;117(1):52-60.
6. Fleming I, Fisslthaler B, Dixit M, Busse R. Role of PECAM-1 in the shear-stress-induced activation of Akt and the endothelial nitric oxide synthase (eNOS) in endothelial cells. *J Cell Sci* 2005;118(18):4103-4111.
7. McCarty OJT, Larson MK, Auger JM et al. Rac1 is essential for platelet lamellipodia formation and aggregate stability under flow. *J Biol Chem* 2005;280(47):39474-39484.

8. Busse R, Lamontagne D. Endothelium-derived bradykinin is responsible for the increase in calcium produced by angiotensin-converting enzyme inhibitors in human endothelial cells. *Naunyn Schmiedebergs Arch Pharmacol* 1991;344(1):126-129.
9. Mause SF, von Hundelshausen P, Zernecke A, Koenen RR, Weber C. Platelet microparticles: a transcellular delivery system for RANTES promoting monocyte recruitment on endothelium. *Arterioscler Thromb Vasc Biol* 2005;25(7):1512-1518.

Supplementary Table 1 Metabolic parameters of patients (n=12) whose platelets were used for proteomic analysis after 12 weeks of treatment with either pioglitazone (30 mg/day) or placebo; FPG = fasting plasma glucose, TG = triglycerides, HOMA IR = homeostasis model assessment index of insulin resistance; *P<0.05 versus placebo-treated patients.

	Placebo	Pioglitazone
BMI (kg/m²)	32.8±5.2	32.9±5.5
Weight (kg)	93.7±14.4	94.9±16.3
FPG (mmol/L)	7.7±3.6	5.9±2.3 *
HbA_{1c} (%)	6.5±0.9	6.2±0.9 *
HOMA IR	3.9±4.6	1.8±2.15
TG (mmol/L)	2.2±1.7	1.9±1.0
LDL (mmol/L)	2.6±0.9	2.6±0.9
HDL (mmol/L)	1.3±0.5	1.3±0.7
Systolic BP (mmHg)	144±18	133±17
Diastolic BP (mmHg)	69±11	67±11

Supplementary Table 2 Details of concomitant disease and medication in the platelet proteomics patient population.

Concomitant disease	Male	Female
Hypertension	8	5
Hyperlipidemia	7	5
Hyperuricemia	2	
Concomitant medication		
ACE-inhibitor or AT blocker	7	4
Beta-Blocker	5	2
Ca-channel Blocker	5	3
diuretic	3	3
Other antihypertensive	3	1
Insulin	7	5
Sulphonylurea	3	
Metformin	1	
CSE inhibitor	7	5
Proton pump inhibitor	3	1

Supplementary Table 3. Proteins identified by MS as being altered by pioglitazone treatment. List of proteins identified among the 63 differentially expressed protein spots picked for analysis as indicated in supplemental Figure 1. Criterion for inclusion included at least a ±1.2 fold change in all of the patients studied and P<0.05.

No.	Protein name	Accession numbers	Mw (Da)	# unique peptides	Number of unique spectra	Number of total spectra	Percentage of total spectra	Percentage sequence coverage	Paired T-test	Paired Ratio	Av
1	Talin-1	TLN1_HUMAN	269.747	24	29	48	5,18%	12,20%	0,023		-1,58
2	Filamin-A	FLNA_HUMAN	280.711	40	46	72	5,53%	20,10%	0,022		-1,49
2	Talin-1	TLN1_HUMAN	269.747	27	34	56	4,30%	13,70%	0,022		-1,49
2	Vinculin	VINC_HUMAN	123.783	25	29	51	3,92%	23,40%	0,022		-1,49
3	Filamin-A	FLNA_HUMAN	280.711	30	36	55	6,72%	14,00%	0,016		-1,66
3	Talin-1	TLN1_HUMAN	269.747	20	23	36	4,40%	9,80%	0,016		-1,66
3	Vinculin	VINC_HUMAN	123.783	21	22	37	4,52%	20,80%	0,016		-1,66
4	Filamin-A	FLNA_HUMAN	280.711	24	27	39	4,34%	11,20%	0,0089		-1,77
4	Talin-1	TLN1_HUMAN	269.747	14	14	22	2,45%	6,85%	0,0089		-1,77
4	Vinculin	VINC_HUMAN	123.783	22	24	37	4,12%	21,20%	0,0089		-1,77
5	Talin-1	TLN1_HUMAN	269.747	24	31	49	5,54%	12,00%	0,017		-1,27
6	Programmed cell death 6-interacting	PDC6I_HUMAN	96.007	16	16	26	2,91%	18,00%	0,013		-1,42
7	Thrombospondin-1	TSP1_HUMAN	129.364	13	15	25	2,92%	13,20%	0,0021		1,51
8	Vinculin	VINC_HUMAN	123.783	22	25	60	5,20%	22,50%	0,013		1,8
9	Talin-1	TLN1_HUMAN	269.747	29	37	124	8,11%	15,70%	0,0058		-1,45
10	Talin-1	TLN1_HUMAN	269.747	42	55	181	9,84%	19,90%	0,0066		-1,39
11	Talin-1	TLN1_HUMAN	269.747	39	47	153	9,71%	19,60%	0,0055		-1,46
12	Talin-1	TLN1_HUMAN	269.747	20	20	71	19,20%	9,33%	0,034		-1,33
13	Filamin-A	FLNA_HUMAN	280.711	19	21	36	5,22%	7,86%	0,011		-1,42
14	Talin-1	TLN1_HUMAN	269.747	28	35	102	5,84%	14,10%	0,0031		-1,37
15	Talin-1	TLN1_HUMAN	269.747	19	24	50	3,86%	9,29%	0,0019		-1,29
16	Glycerol-3-phosphate dehydrogenase,	GPDM_HUMAN	80.818	17	20	38	2,88%	25,90%	0,041		-1,23
17	Fibrinogen alpha chain	FIBA_HUMAN	94.955	17	22	43	3,47%	20,00%	0,036		-1,25
18	Fibrinogen alpha chain	FIBA_HUMAN	94.955	19	26	61	4,71%	21,50%	0,032		-1,28
19	Fibrinogen alpha chain	FIBA_HUMAN	94.955	18	25	69	5,24%	22,60%	0,048		-1,3
20	Fibrinogen alpha chain	FIBA_HUMAN	94.955	17	25	47	3,15%	22,70%	0,023		-1,28
20	Gelsolin	GELS_HUMAN	85.680	13	16	35	2,35%	20,80%	0,023		-1,28
21	Fibrinogen alpha chain	FIBA_HUMAN	94.955	18	24	56	5,13%	21,90%	0,028		-1,36
22	Fibrinogen alpha chain	FIBA_HUMAN	94.955	12	18	33	3,68%	16,30%	0,027		-1,31
23	Alpha-actinin-1	ACTN1_HUMAN	103.043	8	9	11	0,88%	8,86%	0,025		1,26
23	Integrin alpha-IIb	ITA2B_HUMAN	113.373	7	7	10	0,80%	7,31%	0,025		1,26
23	Neutral alpha-glucosidase AB	GANAB_HUMAN	106.858	7	7	12	0,96%	7,52%	0,025		1,26
24	Filamin-A	FLNA_HUMAN	280.711	14	14	25	2,46%	7,48%	0,026		-1,37
24	Talin-1	TLN1_HUMAN	269.747	12	12	19	1,87%	6,34%	0,026		-1,37
24	Thrombospondin-1	TSP1_HUMAN	129.364	9	9	16	1,57%	8,21%	0,026		-1,37
24	Vinculin	VINC_HUMAN	123.783	12	12	22	2,16%	12,60%	0,026		-1,37
25	Filamin-A	FLNA_HUMAN	280.711	27	31	47	4,39%	11,90%	0,021		1,29
25	Talin-1	TLN1_HUMAN	269.747	16	20	28	2,62%	8,46%	0,021		1,29
26	Talin-1	TLN1_HUMAN	269.747	21	25	63	5,18%	10,00%	0,033		-1,3
27	Moesin	MOES_HUMAN	67.804	5	6	8	0,90%	8,32%	0,0075		-1,42
27	Serum albumin	ALBU_HUMAN	69.349	13	13	20	2,24%	18,90%	0,0075		-1,42
28	Fibrinogen alpha chain	FIBA_HUMAN	94.955	15	20	32	3,78%	17,90%	0,045		-1,25
29	Fibrinogen alpha chain	FIBA_HUMAN	94.955	12	17	23	2,68%	16,30%	0,026		-1,22
30	RUN and FYVE domain-containing	RUFY1_HUMAN	79.801	6	7	11	1,02%	9,46%	0,017		-1,34
30	von Willebrand factor	VWF_HUMAN	309.268	5	5	6	0,55%	2,03%	0,017		-1,34
31	Fibrinogen gamma chain	FIBG_HUMAN	51.495	27	38	148	6,68%	74,40%	0,00083		-1,26
32	Phosphoglucomutase-1	PGM1_HUMAN	61.433	9	11	18	1,41%	16,90%	0,016		-1,21
32	Tubulin beta-2A chain	TBB2A_HUMAN	49.889	5	6	15	1,18%	12,10%	0,016		-1,21
33	Fibrinogen gamma chain	FIBG_HUMAN	51.495	17	20	57	4,40%	41,70%	0,046		-1,22
34	Fibrinogen gamma chain	FIBG_HUMAN	51.495	19	23	86	4,82%	45,50%	0,031		-1,28
35	Fibrinogen beta chain	FIBB_HUMAN	55.911	10	14	33	3,40%	22,20%	0,044		-1,24
36	Adenosylhomocysteinase	SAHH_HUMAN	47.699	5	5	8	0,64%	11,80%	0,015		-1,27
36	Tubulin beta-1 chain	TBB1_HUMAN	50.309	7	7	11	0,88%	17,30%	0,015		-1,27
37	Fibrinogen beta chain	FIBB_HUMAN	55.911	5	5	9	1,10%	13,80%	0,044		-1,24
37	Pyruvate kinase isozymes M1/M2	KPYM_HUMAN	57.920	5	5	5	0,61%	10,20%	0,044		-1,24
37	Septin-5	SEPT5_HUMAN	42.760	6	7	13	1,59%	15,70%	0,044		-1,24
38	Unidentified	-	-	-	-	-	-	-	0,011		-1,44
39	Tubulin alpha-1A chain	TBA1A_HUMAN	50.118	12	18	87	4,62%	26,20%	0,018		-1,27
40	PDZ and LIM domain protein 1	PDLI1_HUMAN	36.053	16	23	64	5,46%	49,20%	0,035		-1,88
41	Alpha-enolase	ENOA_HUMAN	47.152	8	9	18	2,01%	21,90%	0,022		1,27
42	PDZ and LIM domain protein 1	PDLI1_HUMAN	36.053	9	14	27	4,88%	29,80%	0,048		-1,81
43	Tubulin beta-1 chain	TBB1_HUMAN	50.309	9	10	26	2,76%	18,80%	0,039		1,21
44	Actin-related protein 2/3 complex	ARPC2_HUMAN	34.316	5	5	8	0,73%	19,70%	0,0079		-1,27
44	Glyceraldehyde-3-phosphate	G3P_HUMAN	36.035	5	7	13	1,19%	17,30%	0,0079		-1,27
45	Filamin-A	FLNA_HUMAN	280.711	5	7	9	1,27%	1,89%	0,0073		1,49
46	Heat shock protein beta-1	HSPB1_HUMAN	22.765	5	5	5	0,83%	28,80%	0,014		1,84
46	Peroxiredoxin-6	PRDX6_HUMAN	25.018	6	6	8	1,32%	29,50%	0,014		1,84
47	Protein ETHE1, mitochondrial	ETHE1_HUMAN	27.855	6	7	11	1,27%	28,30%	0,012		1,49
48	Integrin-linked protein kinase	ILK_HUMAN	51.402	5	5	15	1,78%	12,40%	0,0058		1,32
48	Peroxiredoxin-1	PRDX1_HUMAN	22.093	6	6	10	1,19%	33,20%	0,0058		1,32
49	Fibrinogen gamma chain	FIBG_HUMAN	51.495	6	7	11	1,32%	15,20%	0,049		-1,2
50	Transgelin-2	TAGL2_HUMAN	22.374	16	19	75	4,54%	83,40%	0,0012		-1,67
51	Galectin-related protein	LEGL_HUMAN	18.968	5	5	13	1,16%	23,80%	0,028		-1,21
51	Tubulin beta-1 chain	TBB1_HUMAN	50.309	5	6	21	1,87%	12,00%	0,028		-1,21
52	Fibrinogen gamma chain	FIBG_HUMAN	51.495	6	8	38	3,16%	19,00%	0,0015		-1,64
52	Peroxiredoxin-6	PRDX6_HUMAN	25.018	5	5	7	0,58%	22,80%	0,0015		-1,64
53	Histidyl-tRNA synthetase, cytoplasmic	SYHC_HUMAN	57.394	7	7	9	1,00%	12,60%	0,0038		-1,57
54	Tropomyosin alpha-3 chain	TPM3_HUMAN	32.802	5	7	17	1,81%	10,60%	0,0059		-1,34
55	Tropomyosin alpha-1 chain	TPM1_HUMAN	32.692	5	5	9	0,86%	12,30%	0,0017		-1,3
55	Tropomyosin alpha-3 chain	TPM3_HUMAN	32.802	6	9	17	1,63%	15,10%	0,0017		-1,3
56	Unidentified	-	-	-	-	-	-	-	0,016		-1,23
57	Unidentified	-	-	-	-	-	-	-	0,048		1,4
58	Unidentified	-	-	-	-	-	-	-	0,0073		-1,22
59	Unidentified	-	-	-	-	-	-	-	0,0013		1,25
60	Unidentified	-	-	-	-	-	-	-	0,0096		1,52
61	Platelet basic protein	CXCL7_HUMAN	13.877	11	15	74	5,28%	57,80%	0,023		1,68
62	Filamin-A	FLNA_HUMAN	280.711	14	17	95	4,50%	3,93%	0,012		1,29
63	Filamin-A	FLNA_HUMAN	280.711	5	6	27	3,44%	2,04%	0,0068		1,48

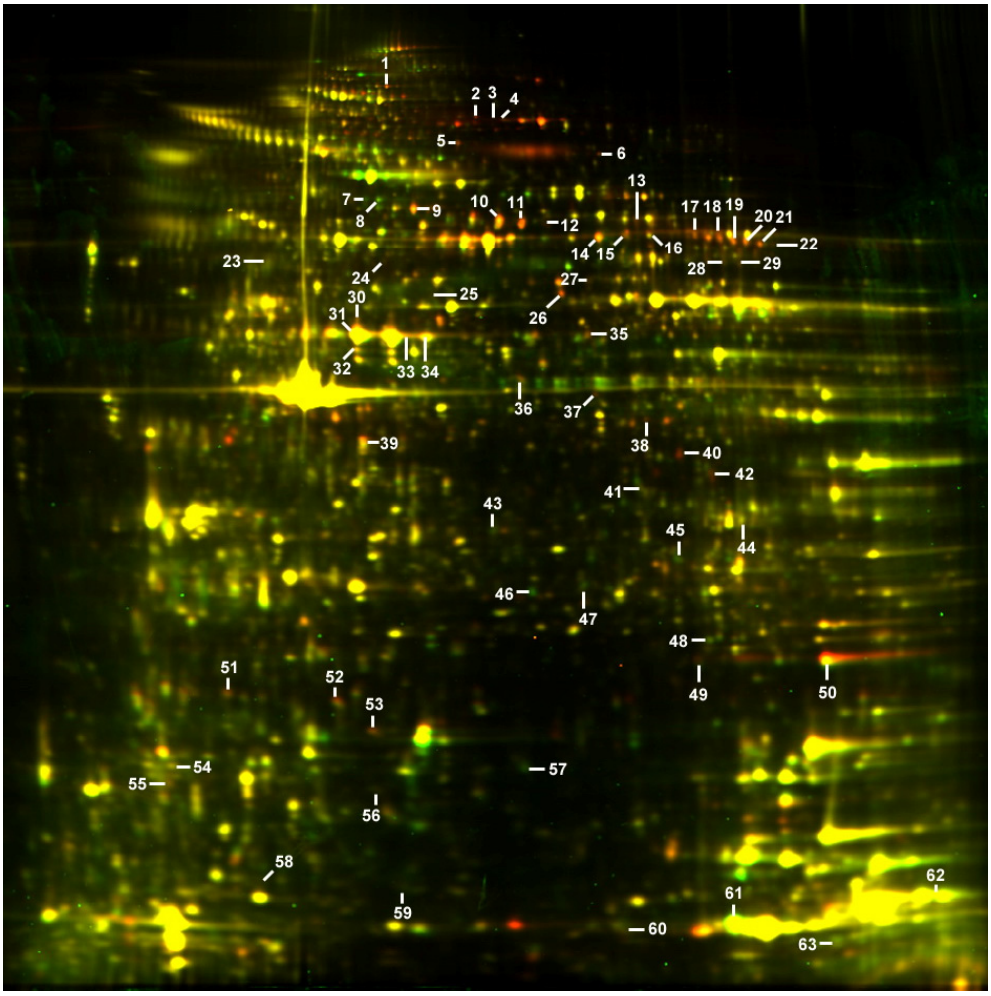

Supplemental Figure 1. 2D-DIGE proteome analysis of platelets from diabetic individuals before and after treatment with placebo or pioglitazone (30 mg/day, 12 weeks). The figure shows the location of the spots picked for MS analysis (see table S2 for identity). Green= upregulated in the pioglitazone group compared to controls, red = downregulated in the pioglitazone group compared to controls. Comparable results were obtained in samples from 5 additional subjects.

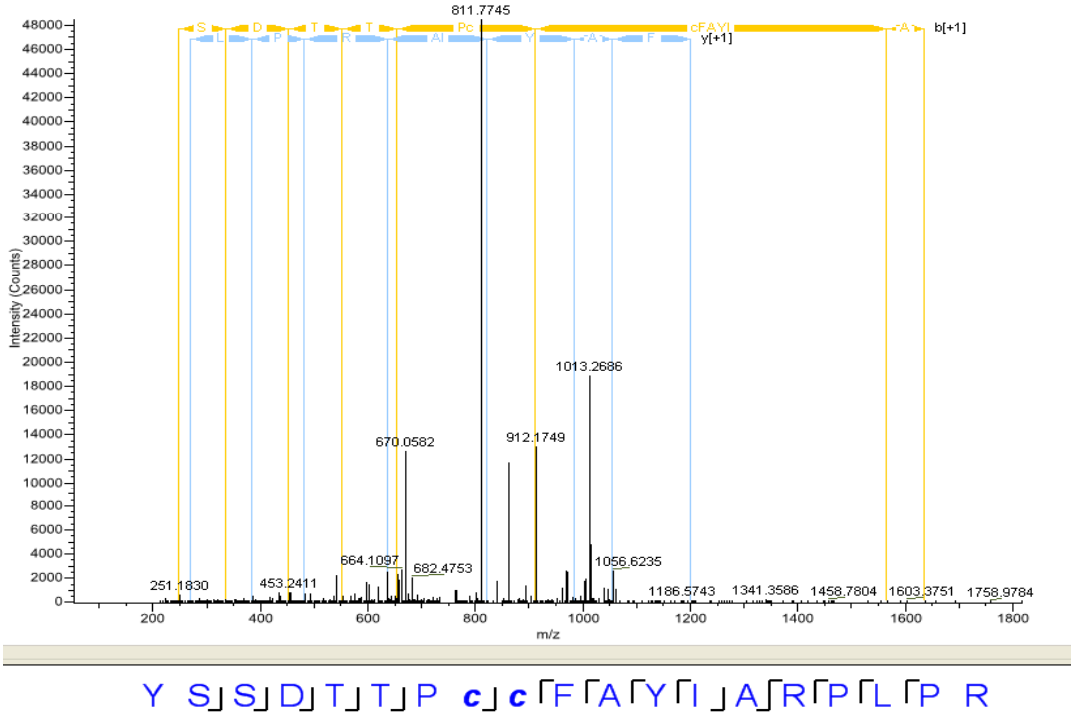

Supplemental Figure 2. MS analysis of calpain cleaved CCL5. MS/MS spectra identifying peptide YSSDTTPCCFAYIARPLPR of CCL5 in μ-calpain treated sample. Charge: +3, monoisotopic m/z: 759.02625 (+0.3 ppm), MH+: 2275.06418 Da, Mascot Ion Score: 51.

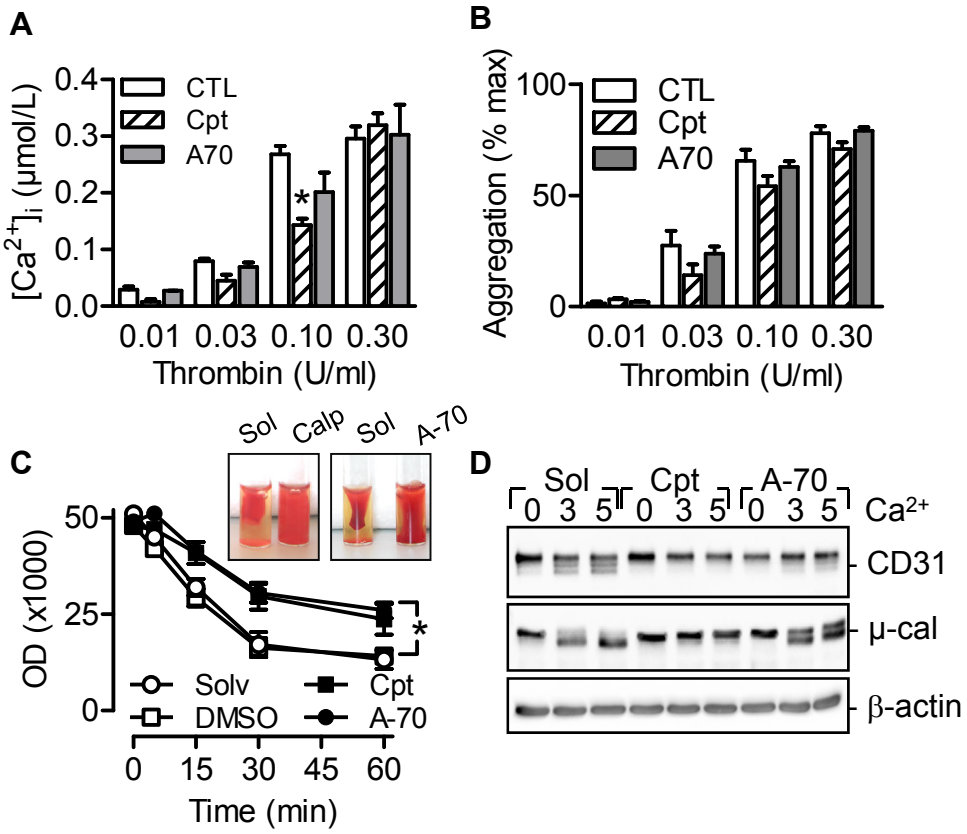

Supplemental Figure 3. Effect of calpain inhibition on platelet function. Washed human platelets were pretreated with either solvent (Sol) calpeptin (Calp, 10 μmol/L) or A- 705253 (A-70, 10 μmol/L) before (**A**) the Ca^{2+} response to thrombin, (**B**) platelet aggregation and (**C**) clot retraction were assessed. The graphs summarise the data from 4-6 different donors; *P<0.05. (**D**) Effect of calpain inhibition on calpain and CD31 levels. Washed human platelets were pretreated with either solvent (Sol) calpeptin (Calp, 10 μmol/L) or A-705253 (A-70, 10 μmol/L) before being stimulated with Ca^{2+} (3 or 5 mmol/L, 30 minutes). Thereafter, the degradation of CD31 and autolytic cleavage of μ- and m-calpain were assessed by Western blotting. Identical results were obtained in 6 additional experiments.

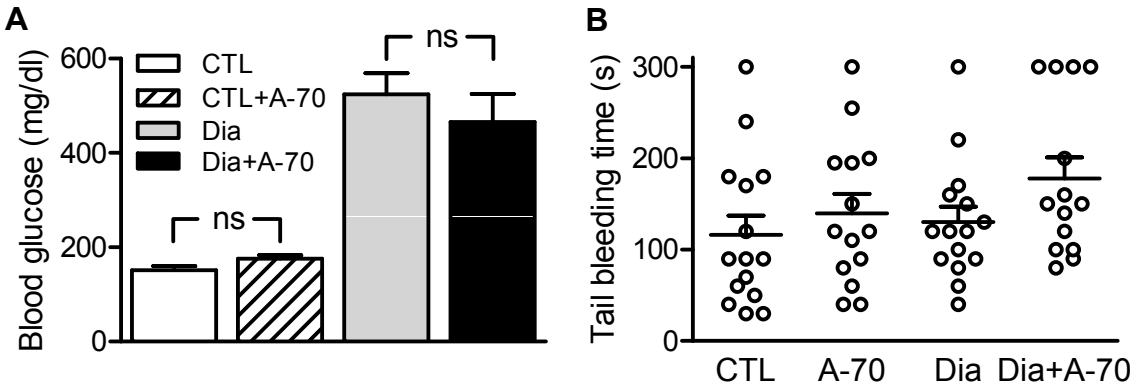

Supplemental Figure 4. Effect of A-705253 on plasma glucose and tail bleeding time. Animals were made diabetic using streptozocin (150mg/kg)) and after 10 weeks were treated with A-705253 (30 mg/kg/day, p.o.) for 12 days. Twenty four hours prior to sacrifice blood samples were taken to assess (**A**) plasma glucose and (**B**) tail bleeding time. The graphs summarise the data from 10-15 mice per group.

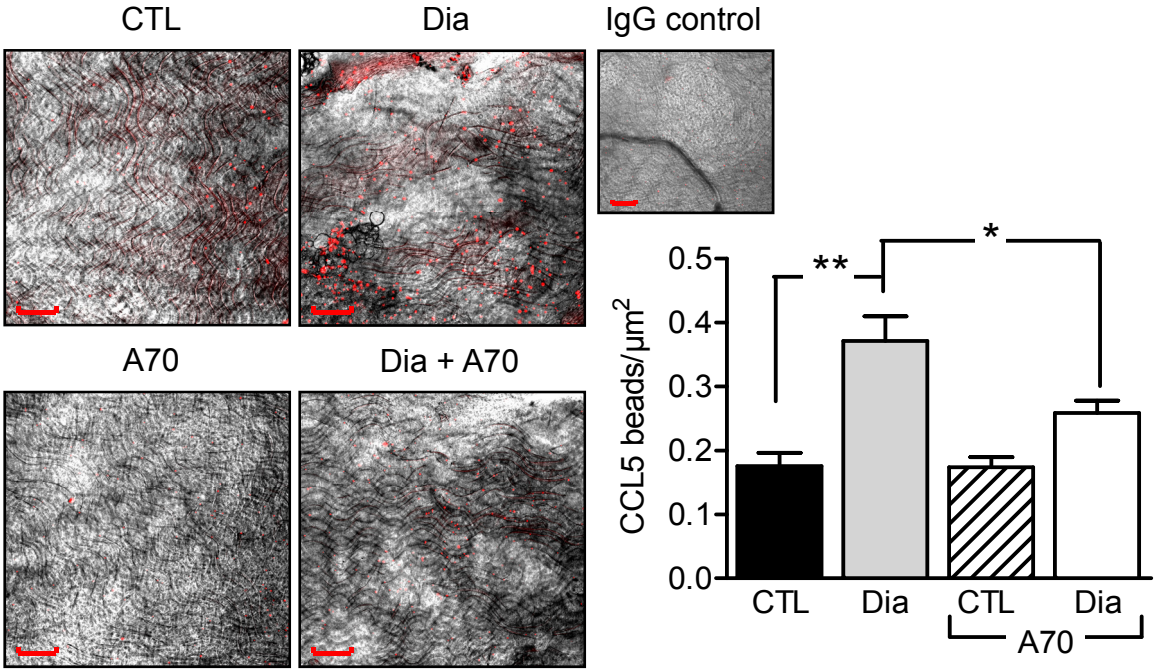

Supplemental Figure 5. *En face* immunofluorescence images showing the effect of A-705253 on CCL5 deposition on carotid arteries from healthy and diabetic mice. Animals were made diabetic using streptozocin (150 mg/kg) and after 12 weeks were treated with A-705253 (A67; 30 mg/kg/day, p.o.) for 12 days. Carotids were isolated and *en face* staining was performed *in situ* with anti-CCL5 antibody coupled to Protein G green fluorescent beads. The insert shows the IgG control; bar = 100 µm. The graph summarizes the data from 5 mice per group.